Screening of Q-markers for the wine-steamed Schisandra chinensis decoction pieces in improving allergic asthma

Zhongyuan Qu
Harbin University of Commerce
Yifan Bing
Harbin University of Commerce
Tianlei Zhang
Harbin University of Commerce
Yan Zheng
Harbin University of Commerce
Shuang Wu
Harbin University of Commerce
Chenfeng Ji
Harbin University of Commerce
Wenlan Li
Harbin University of Commerce
Xiang Zou (zouxiang@hrbcu.edu.cn)
Harbin University of Commerce

Research Article

Keywords: Wine-steamed Schisandra chinensis, Decoction pieces, Quality markers, Allergic asthma, UPLC-Q-TOF-MS/MS

Posted Date: November 4th, 2022

DOI: https://doi.org/10.21203/rs.3.rs-2206738/v1

Abstract

Background

Traditional Chinese medicine (TCM) posits that Chinese medicinal materials can only be used for clinical use after being processed and prepared into decoction pieces. Schisandra Chinensis Fructus (derived from the dried and mature fruits of *Schisandra chinensis* (Turcz.) Baill.) has been traditionally used as an antiasthmatic, kidney strengthening, and hepatoprotective agent for 2000 years. TCM clinic believes that the decoction pieces of wine-steamed Schisandra chinensis (WSC) is advantageous over the raw decoction pieces of Schisandra chinensis (RSC) for cough and asthma. Studies have shown that steaming with wine can promote the dissolution of ingredients. However, the relationship between the changes of components in the decoction pieces of WSC and the therapeutic effect remains unclear.

Methods

The efficacy of the decoction of RSC and WSC were compared based on allergic asthma rats. The potential bioactive components in the serum of the WSC treatment group and the changes of chemical composition in the decoction pieces before and after wine steaming were determined by ultra-performance liquid chromatography quadrupole time-of-flight mass (UPLC-Q-TOF-MS/MS) analysis to speculate quality markers (Q-markers) related to the efficacy of WSC, which was further verified based on the zebrafish model of inflammation.

Results: The results indicated the effect of RSC decoction pieces in improving allergic asthma was increased after being steamed with wine. Moreover, 12 components were detected in the serum of the WSC treatment group, which were conjectured to be the potential effective components. Among them, 5 components, such as Schisandrin, Schisandrol B, Schisandrin A, Schisandrin B, and Gomisin D, have higher dissolution rates than RSC after steaming with wine. The validation test based on the inflammatory zebrafish model showed that these 5 ingredients exerted their effects in a dose-dependent manner, demonstrating that they were Q-markers for WSC in the treatment of allergic asthma.

Conclusion: This study clarified the changes of components of the decoction pieces of RSC and WSC and the Q-markers related to the WSC efficacy, which provide precious value for expanding the application of WVS and establishing its exclusive quality standard.

Introduction

Bronchial asthma, the most common chronic respiratory inflammatory disease globally, is characterized by wheezing, shortness of breath, or coughing [1]. Up to now, 241 million people in various countries are subject to asthma, and the morbidity in Asian and western countries is expected to continue to rise [2, 3]. Asthma has the highest proportion of deaths among patients aged 65 and over [4]. Currently, due to the drugs commonly used to treat asthma clinically, such as inhaled corticosteroids, long-acting bronchodilators, and so on, are often accompanied by obvious side effects [5], Researchers began to discover novel anti-asthma natural medicinal resources.

Schisandra Chinensis Fructus (the dried and mature fruits of *Schisandra chinensis* (Turcz.) Baill.) was first recorded in *Shennong's Herbal Classic of Materia Medica* and is widely applied for the treatment of asthma, liver disease, and insomnia [6–8]. In addition to 12 ancient prescriptions for the treatment of Cold Pathogenic and Miscellaneous diseases containing RSC recorded in *Compendium of Materia Medica*, a classic work being regarded as a treasure of pharmacy published about 2000 years ago, increasing evidence indicates that RSC reveals curative effects on asthma [9, 10]. Previous studies on RSC have led to the discovery of several kinds of constituents, including dibenzocyclooctadiene lignans [11], organic acid [12], polysaccharides [13], and volatile oil [14]. Among them, lignans like Deoxyschizandrin, Schisantherin A, Schisandrin B, and

Schisandrin are the most biologically effective components for the effects including antitussive, expectorant, and anti-inflammation [15].

TCM decoction pieces refer to the finished product which is further processed from the original Chinese medicinal materials according to the needs of clinical preparations of TCM under the guidance of the theory of TCM. As one of the characteristics of TCM, processing has the function of reducing toxicity, strengthening the bioactivities, or modifying the nature of medicinal materials. Among them, stir-frying with vinegar or wine, and steaming with water or rice wine are one of the most commonly used processing methods [16, 17]. It is believed that many chemical reactions, such as hydrolysis, oxidation, and decomposition, will occur between medicinal materials and auxiliary materials during processing [18], which is the reason for the difference in efficacy between original medicinal materials and processed pieces. According to the theory of TCM, yellow rice wine has strong antioxidant activity, which can promote the dissolution and absorption of the ingredients and improve the curative effect [19]. Therefore RSC is often used to treat allergic asthma after being prepared into wine steamed decoction pieces [20]. Furthermore, it can be inferred that wine steaming has a significant effect on the efficacy and composition of RSC.

Decoction is one of the most common forms of Chinese medicine in clinical administration, which exhibited remarkable curative effect and has a history of thousands of years. The components contained in decoction are the main components of clinical efficacy. Many scholars have conducted a systematic analysis of the chemical components in the ethanol extract of RSC [21, 22]. However, it is still unclear what components can be extracted in the decoction and what components can be absorbed into the blood for effect, making it difficult to form a specific quality evaluation standard for decoction pieces. Therefore, in order to establish the exclusive quality evaluation standard for WSC decoction pieces, we screened the active components of WSC decoction pieces based on allergic asthma model, determined the Q-marker related to WSC efficacy by comparing the composition changes of RSC and WSC decoction pieces, and verified the screening results of Q-marker by zebrafish. The graphic abstract was shown in Fig. 1.

Materials And Methods

Materials and Reagents

Eight standard compounds in Schisandrae Chinensis Fructus with a purity > 98% were obtained from Chengdu Institute of Biology, Chinese Academy of Sciences (Chengdu, China), including Schisandrin A, Schisandrin B, Schisanhenol, Gomisin D, Schisandrol B, Schisandrin, Schisantherin B and Schisantherin A. OVA was bought from Beijing Boao Biological Co., Ltd. (Beijing, China). Aluminum hydroxide and Bailing capsules were purchased from Hangzhou Zhongmei Huadong Pharmaceutical Co., Ltd. (Hangzhou, China). HPLC-grade acetonitrile and methanol were provided by Merck (Darmstadt, Germany). Formic acid (HPLC-grade) was collected from Thermo-Fisher (New York, US). Water for LC-MS analysis was acquired from Watsons (Guangzhou, China). Dexamethasone (Dex) and Tricaine were supported by Sigma-Aldrich(Darmstadt, Germany). ELISA kits were all produced by Shanghai Guangrui Biotechnology Co., Ltd. (Shanghai, China).

Animals

90 male SD rats weighing 180 ± 20g were provided from Changchun Yisi Experimental Animal Technology Co., Ltd. (Changchun, China; License No: 2018095). All the rats were randomly housed in temperature-controlled cages under 50% ±10% humidity and a 12 h light-dark cycle. They were acclimated for one week before the experiment, which was approved by The Animal Ethics Committee of the School of Pharmacy, Harbin University of Commerce (HSDYXY2018025).

490 adult AB strain zebrafish were purchased from the National Zebrafish Resource Center and housed in a circular culture system in our laboratory as stated in Zebrafish Book [23] at a water temperature of 28 ± 0.5 ℃ and a dark/photoperiod of 10 h/14 h.

Preparation of RSC and WSC extract

Schisandrae Chinensis Fructus was collected from Heilongjiang province, confirmed by Professor Jin Zhexiong from the School of Pharmacy, Harbin University of Commerce. WSC was prepared as follows: RSCs were mixed with wine in a sealed container for 1 h (5:1. RSC: wine, M: V), then steamed until the wine was absorbed completely and dried at 60℃ .

The dried RSC or WSC decoction pieces were soaked respectively for 30 min before decocting with 10 times the amount of water for 30 min in the first time and 8 times the amount of water for 20 min in the second time. After filtering with silk cloth, the cooking liquid was combined twice and concentrated to a concentration of 1g/mL.

Rat experiments

Allergic asthma model was induced according to the previous report [24]. 90 SD rats were randomly selected and divided into 9 groups (n = 10) : normal group, model group, positive drug group (Bailing capsule, 0.92 g/kg/d), RSC, WSC high-dose, medium-dose and low-dose groups, respectively. Except the control group, the other rats were intraperitoneally injected 1 mL/d a suspension of sodium chloride solution (containing OVA (60 mg, 5%) and 100 mg (10%) aluminum hydroxide gel) intraperitoneally at 1 and 8 days to conduct sensitization test. From day 9 to day 28, rats that had been sensitized to OVA were challenged with 1% aerosolized OVA to construct the asthma model. The normal group was given 0.9% normal saline daily. The administration group was given corresponding drugs by gavage. General behavior was observed 1 h after the last dose. Based on clinical research, RSC is often decocted at a dose of 6-15g in the treatment of asthma and wheezing cough [25]. Therefore, 15g was selected as the one-fold dose in this study, and 1/2-fold, 1-fold, and 2-fold dose groups were respectively set up, which were converted to 0.77 g/kg, 1.54 g/kg, and 3.09 g/kg as the daily intake of rats. Therefore, the the dosage of RSC and WSC in high, medium and low dose groups were 3.09 g/kg, 1.54 g/kg, and 0.77 g/kg, respectively.

Enzyme-linked immunosorbent assay (ELISA)

Briefly, 6 8 mL blood samples were collected after being euthanized for the determination of indicators on the one hand, and identification of the absorbed components into the blood on the other hand. The supernatant from each specimen was collected for ELISA to quantify the immunoglobulin E (IgE), interferon γ (IFN-γ), and interleukin 4 (IL-4), content by centrifugation at 3000 rpm for 15 min at 4℃.

Histology Staining

After blood collection, the lungs were removed for for pathological examination. Briefly, upon fixation in 10% formaldehyde solution, paraffin embedding, sectioning, and dewaxing, the lungs were stained with hematoxylin-eosin (HE) for observation.

Preparation of serum samples

Blood of blank group and WSC-H group for serum pharmacochemistry was treated with methanol and transferred to UPLC-Q-TOF-MS/MS for analysis. Briefly, Serum proteins were precipitated by adding methanol (1:3 serum: methanol) at 4℃ and centrifuging for 10 min at 4000rpm. Following centrifugation to remove proteins, the supernatant was evaporated under nitrogen at 35 ℃, dissolved with 200 μL of methanol, and filtered (0.22 μm pore size) for UPLC-Q-TOF-MS/MS analysis.

Chromatographic and mass spectrometric conditions

Chromatographic separation was carried out on a UPLC HSS T3 column (Waters, Milford, 1.8 μm×100 mm×2.1 mm, USA) using a 28-min gradient with the flow of 0.2 mL/min and an injection volume of 5 μL. The column temperature was 35 ℃. The mobile phase consisted of deionized water with 0.1% formic acid (A) and acetonitrile (B). The gradient elution was as follows: 0–3 min, 0%-23%B;3–7 min, 23%-40%B 7–8 min, 40%-42%B; 8-11.5 min, 42%-55%B; 11.5–13 min, 55%-65%B; 13-14.5 min, 65%-75%B; 14.5–19 min, 75%-100%B; 19–28 min, 100%-23%B.

The mass analysis was operated on Agilent G6545 Q-TOF mass spectrometer (Agilent, USA) in positive and negative ion modes within the mass range of m/z 80 1500. The optimized ESI conditions were as follows: collision energy, 35 ev

(positive ion mode) and − 35 ev (negative ion mode); curtain gas (N_2), 35 psi; sheath gas (N_2), 55 psi; auxiliary gas (N_2), 5 psi; ion spray voltage, 5.5 kV (positive ion mode) and 4.5 kV (negative ion mode); collision energy spread, 15 eV. The error limit of retention time and mass was set to 0.01 min and 0.01 Da, respectively.

Systematic analysis of metabolites in serum samples

A database containing English names, molecular formulas, molecular weights, and structural formulas of all compounds and metabolic ingredients in RSC was established by collecting Chinese and English literature and searching PubChem, TCMSP, ChemSpider, and other databases. The original serum data of the WSC-H administration group obtained from the analysis were imported into MakerView software, and the conditions were used as the standard for data screening, with the condition that error limit of retention time of 0.01 minutes, and mass error limit of 0.01 Da. Whereafter, the established RSC compositions and metabolic ingredients database was imported into MakerView software. According to the matching results, compositions in the serum of the WSC-H administration group were identified by analyzing the cleavage characteristic.

UPLC-Q-TOF-MS/MS analysis of RSC and WSC extract

Preparation of mixed standard: The stock of Schisandrin A, Schisandrin B, Schisanhenol, Gomisin D, Schisandrol B, Schisandrin, Schisantherin B, and Schisantherin A standards was prepared in acetonitrile and the concentration was 0.2 mg/mL. All samples were filtered through a 0.22 μm microporous membrane for standby.

Preparation of decoction samples: After being extracted following the operation in “Preparation of RSC and WSC extract”, RSC and WSC samples were concentrated and redissolved in 25 mL highly pure acetonitrile to the concentration of 0.04 g/mL. The UPLC-Q-TOF-MS/MS analysis was performed according to the above chromatographic and mass spectroscopic conditions.

Data analysis: The original RSC and WSC data obtained from the analysis were imported into MakerView software and analyzed according to the method of serum sample data analysis method.

Multivariate statistical analysis

Principal component analysis (PCA) aims to extract a few principal components from multiple indicators through dimensionality reduction while maintaining as much information as possible. Specifically, six samples of the same batch of RSC and WSC were prepared, and the obtained sample data were imported into MakerView software for data analysis to obtain PCA score-plot and loading-plot to screen the differential chemical components. The selected components were identified by comparing the literature and the MakerView software.

Validation of monomeric components based on zebrafish inflammation model

Determination of maximum tolerance concentration (MTC): 260 healthy adult zebrafish with similar body sizes were randomly selected and divided into the normal group, Schisandrin, Schisandrol B, Schisandrin A, Schisandrin B, and Gomisin D treatment groups. Each treatment group was divided into 5 groups pursuant to the concentration of 10μM, 20μM, 40μM, 80μM, and 160μM, respectively, with 10 fish in each group. After 24 hours of culture, the number of deaths in each group was counted to determine MTC. Subsequently, the MTC value was set as the high dose, 1/2 MTC as the medium dose, and 1/4 MTC as the low dose for each administration group.

Tail transection and screening of administration time points: A total of 50 adult zebrafish were divided into 5 groups, including a normal group, model group (tail transection for 1 h), model group (tail transection for 2 h), model group (tail transection for 4 h), and model group (tail transection for 6 h), with 10 fish in each group. The model group was anesthetized in water containing 0.1% tricaine and the tail was cut off on a triangular plate covered with 2% agarose with a sterile scalpel (to avoid injury to the spinal cord) [26]. After amputation, zebrafish were placed in water at 28.5 °C to

continue culture for the corresponding time. At the end of the experiment, 10 zebrafish in each group were anesthetized in an ice water bath, and the tissue was cut with sterile surgical scissors and added into pre-cooled 0.9% normal saline at the ratio of 1:9 (m/m) into the homogenizer for grinding. After preparation, the homogenate was centrifuged at 2500 r/min for 10min to obtain supernatants to determine the expression levels of tumor necrosis factor-α (TNF-α), interleukin 6 (IL-6), and interleukin 10 (IL-10). The point with the highest expression of inflammatory factors was selected as the best time point for research.

Efficacy validation: A total of 180 adult zebrafish were divided into 18 groups with 10 for each: the normal group, model group, positive drug group (10 μM Dex [27]), high, medium, and low dose groups of each component. The zebrafish inflammation model was established through tail amputation in the other groups except for the normal group. After tail transection, the zebrafish were treated with drugs for 2 h respectively and the level of TNF-α, IL-6, and IL-10 was measured.

Data analysis

Statistical analyses were conducted using SPSS software v21.0 (SPSS Corporation, Chicago, Illinois, US) and presented as mean ± SD. Shapiro-Wilk test was used to verify whether the data follow the normal distribution. Data conforming to normal distribution was further analyzed using one-way ANOVA to access the difference in variability between groups.

Results

The effect of WSC in improving allergic asthma was more potent than RSC at the same dose

The general behavior of rats in all groups was monitored after the last dose. It was found that OVA atomization led to allergic asthma, manifested as classical shortness of breath, panting, wheezing, and sneezing, which implied the successfully-establishment of allergic asthma. After the treatment, the RSC and WSC dose groups exhibited an ameliorative effect, similar to the Bailing capsule, on the symptoms mentioned above, mainly reflected in brighter fur, gradual weight gain, and mental state. Moreover, the mice in RSC-H and WSC-H were in a better state.

Moreover, the serum IFN-γ levels were distinctly reduced in the model group compared to the normal group ($P < 0.01$, Fig. 2B, Table 1), whereas the expression of IL-4 and IgE was higher ($P < 0.01$, Fig. 2B, Table 1), indicating the imbalance of the Th1/Th2 ratio occurred in allergic asthma rats. Both RSC and WSC administration caused the elevation of IFN-γ and the decrease of IL-4 and IgE levels in a dose-dependent manner compared with the model group. Among them, the RSC-H, WSC-H and WSC-M groups had a better efficacy ($P < 0.05$ or $P < 0.01$). Interestingly, it was worth mentioning that the effect of WSC was superior to RSC at the equivalent dose.

Table 1
Identification of potentially bioactive compounds of WSC

No	RT (min)	Adduction	M/Z	ppm	Formula	Fragments	Identification	Type
1	12.4	$[M + H]^+$	433.2223	0.5	$C_{24}H_{32}O_7$	433.1891 $[M + H]^+$, 384.1905 $[M + H\text{-}CH_4O_2]^+$, 369.1672 $[M + H\text{-}CH_4O_2\text{-}CH_3]^+$, 338.1488 $[M + H\text{-}CH_4O_2\text{-}CH_3\text{-}CH_3O]^+$	Schisandrin	prototype
2	15.4	$[M + H]^+$	417.1909	0.5	$C_{23}H_{28}O_7$	417.1815 $[M + H]^+$, 399.1699 $[M + H\text{-}H_2O]^+$, 358.1321 $[M + H\text{-}H_2O\text{-}CH_3\text{-}C_2H_4]^+$, 314.1084 $[M + H\text{-}H_2O\text{-}CH_3\text{-}C_2H_4\text{-}CH_3CO]^+$	Schisandrol B	prototype
3	12.7	$[M + H]^+$	391.2846	0.9	$C_{24}H_{38}O_4$	391.3340 $[M + H]^+$, 279.1769 $[M + H\text{-}7CH_2\text{-}CH_3]^+$, 205. 1174 $[M + H\text{-}7CH_2\text{-}CH_3\text{-}7CH_2\text{-}2CH\text{-}COOH\text{-}2OH]^+$	Merulinic acid A	prototype
4	12.9	$[M + H]^+$	401.1598	1.1	$C_{22}H_{24}O_7$	401.1602 $[M + H]^+$, 352.1309 $[M + H\text{-}OCH_3]^+$, 337.1058 $[M + H\text{-}OCH_3\text{-}CH_3]^+$	Gomisin R	prototype
5	12.9	$[M + H]^+$	531.2229	0.8	$C_{28}H_{34}O_{10}$	531.2152 $[M + H]^+$, 485.2161 $[M + H\text{-}CH_2O_2]^+$, 401.1588 $[M + H\text{-}CH_2O_2\text{-}C_5H_8O]^+$, 383.1488 $[M + H\text{-}CH_2O_2\text{-}C_5H_8O\text{-}H_2O]^+$	Gomisin D	prototype

No	RT (min)	Adduction	M/Z	ppm	Formula	Fragments	Identification	Type
6	14.4	$[M + H]^+$	401.1957	-0.2	$C_{23}H_{28}O_6$	401.1957 $[M + H]^+$, 370.1746 $[M + H\text{-}OCH_3]^+$, 331.1149 $[M + H\text{-}C_5H_{10}]^+$, 316.0927 $[M + H\text{-}CH_3\text{-}C_5H_{10}]^+$, 300.0969 $[M + H\text{-}CH_3\text{-}O\text{-}C_5H_{10}]^+$	Schisandrin B	prototype
7	3.62	$[M + H]^+$	221.0652	-1.5	$C_8H_{12}O_7$	221.0655 $[M + H]^+$, 157.0484 $[M + H\text{-}OH\text{-}COOH\text{-}CH_3]^+$,139.0023 $[M + H\text{-}OH\text{-}COOH\text{-}CH_3\text{-}H_2O]^+$	Dimethyl citrate	prototype
8	15.4	$[M + H]^+$	415.1753	0.5	$C_{23}H_{26}O_7$	415.1742 $[M + H]^+$, 385.1644 $[M + H\text{-}CH_2O]^+$, 371.1481$[M + H\text{-}CH_2O\text{-}CH_3]^+$	Neoisostegane	prototype
9	17.3	$[M + H]^+$	385.1646	0.1	$C_{22}H_{24}O_6$	385.1650 $[M + H]^+$, 355.1546 $[M + H\text{-}OCH_3]^+$, 285.0754 $[M + H\text{-}OCH_3\text{-}C_5H_{10}]^+$	Schisandrin C	prototype
10	10.0	$[M + H]^+$	431.2069	1.1	$C_{24}H_{30}O_7$	431.2033 $[M + H]^+$, 400.1865 $[M + H\text{-}OCH_3]^+$,372.1549 $[M + H\text{-}OCH_3\text{-}C_2H_4]^+$	Schinsanlignone A	prototype
11	8.3	$[M + H]^+$	433.1851	0.8	$C_{23}H_{28}O_8$	433.1851 $[M + H]^+$, 415.1751 $[M + H\text{-}H_2O]^+$, 384.1572 $[M + H\text{-}H_2O\text{-}OCH_3]^+$, 369.1326 $[M + H\text{-}H_2O\text{-}OCH_3\text{-}CH_3]^+$, 345.1315 $[M + H\text{-}H_2O\text{-}C_5H_{10}]^+$, 301.1074 $[M + H\text{-}H_2O\text{-}CO_2\text{-}C_5H_{10}]^+$286.0847 $[M + H\text{-}H_2O\text{-}CO_2\text{-}C_5H_{10}\text{-}CH_3]^+$	6-debenzoyl-Schisantherin A	Metabolites of Schisantherin A

No	RT (min)	Adduction	M/Z	ppm	Formula	Fragments	Identification	Type
12	8.1	$[M + H]^+$	419.1709	0.5	$C_{22}H_{26}O_8$	419.1709 $[M + H]^+$, 401.1632 $[M + H\text{-}H_2O]^+$, 369.1361 $[M + H\text{-}H_2O\text{-}CH_3OH]^+$, 331.1193 $[M + H\text{-}H_2O\text{-}C_5H_{10}]^+$, 316.0941 $[M + H\text{-}H_2O\text{-}C_5H_{10}\text{-}CH_3]^+$	3-demethylation-6-debenzoyl-Schisantherin A	
13	15.5	$[M + H]^+$	415.1760	0.5	$C_{23}H_{26}O_7$	415.1760 $[M + H]^+$, 397.1634 $[M + H\text{-}H_2O]^+$, 385.1650 $[M + H\text{-}OCH_2]^+$, 371.1489 $[M + H\text{-}OCH_2\text{-}CH_3]^+$, 342.1110 $[M + H\text{-}OCH_2\text{-}CH_3\text{-}HCO]^+$, 340.1316 $[M + H\text{-}OCH_2\text{-}CH_2\text{-}OCH_3]^+$	7,8-dehydration-6-debenzoyl-Schisantherin A	
14	15.5	$[M + H]^+$	415.1760	0.5	$C_{23}H_{26}O_7$	415.1760 $[M + H]^+$, 397.1634 $[M + H\text{-}H_2O]^+$, 385.1650 $[M + H\text{-}OCH_2]^+$, 371.1489 $[M + H\text{-}OCH_2\text{-}CH_3]^+$, 342.1110 $[M + H\text{-}OCH_2\text{-}CH_3\text{-}HCO]^+$, 340.1316 $[M + H\text{-}OCH_2\text{-}CH_2\text{-}OCH_3]^+$	7,17-dehydration-6-debenzoyl-Schisantherin A	
15	14.4	$[M + H]^+$	401.1970	0.7	$C_{23}H_{28}O_6$	401.1970 $[M + H]^+$, 386.1740 $[M + H\text{-}CH_3]^+$, 370.1788 $[M + H\text{-}OCH_3]^+$, 369.1720 $[M + H\text{-}CH_3\text{-}OH]^+$, 355.1548 $[M + H\text{-}2CH_3\text{-}OH]^+$	2-demethoxy-Schisandrin A	Metabolites of Schisandrin A

No	RT (min)	Adduction	M/Z	ppm	Formula	Fragments	Identification	Type
16	15.5	$[M + H]^+$	415.1760	0.5	$C_{23}H_{26}O_7$	415.1760 $[M + H]^+$, 397.1634 $[M + H\text{-}H_2O]^+$, 385.1650 $[M + H\text{-}OCH_3]^+$, 371.1498 $[M + H\text{-}OCH_3\text{-}CH_2]^+$, 340.1316 $[M + H\text{-}2OCH_3\text{-}CH_2]^+$, 325.1083 $[M + H\text{-}2OCH_3\text{-}CH_2\text{-}COCH_3]^+$	1-demethoxy-7,8-dicarbonylation-Schisandrin A	
17	8.0	$[M + H]^+$	419.1709	0.9	$C_{23}H_{30}O_7$	419.1709 $[M + H]^+$, 401.1632 $[M + H\text{-}H_2O]^+$, 387.1457 $[M + H\text{-}H_2O\text{-}CH_2]^+$, 369.1361 $[M + H\text{-}H_2O\text{-}CH_2\text{-}H_2O]^+$, 327.1247 $[M + H\text{-}H_2O\text{-}CH_2\text{-}4CH_3]^+$,	3-demethyl-3,7-dihydroxy-Schisandrin A	
18	8.1	$[M + H]^+$	417.1917	0.7	$C_{23}H_{30}O_8$	417.1917 $[M + H]^+$, 399.1777 $[M + H\text{-}H_2O]^+$, 367.1546 $[M + H\text{-}H_2O\text{-}2OH]^+$, 331.1186 $[M + H\text{-}H_2O\text{-}2OH\text{-}2H_2O]^+$, 313.1085 $[M + H\text{-}H_2O\text{-}2OH\text{-}3H_2O]^+$	3-demethyl-3,7,8-trihydroxylated-Schisandrin A	
19	13.2	$[M + H]^+$	389.1957	0.6	$C_{22}H_{28}O_6$	389.1957 $[M + H]^+$, 374.1809 $[M + H\text{-}CH_3]^+$, 357.1713 $[M + H\text{-}CH_3\text{-}OH]^+$, 342.1463 $[M + H\text{-}2CH_3\text{-}OH]^+$, 329.1793 $[M + H\text{-}CH_3\text{-}OH\text{-}CO]^+$, 325.1441 $[M + H\text{-}2CH_3\text{-}OH\text{-}CO]^+$	3,12-dimethyldihydroxy-Schisandrin A	

No	RT (min)	Adduction	M/Z	ppm	Formula	Fragments	Identification	Type
20	8.4	$[M + H]^+$	433.1851	0.8	$C_{23}H_{28}O_8$	433.1851 $[M + H]^+$, 415.1751 $[M + H\text{-}H_2O]^+$, 384.1572 $[M + H\text{-}H_2O\text{-}OCH_3]^+$, 369.1326 $[M + H\text{-}H_2O\text{-}OCH_3\text{-}CH_3]^+$	7-carboxylated - Schisandrin A	
21	12.5	$[M + H]^+$	415.2116	0.7	$C_{24}H_{32}O_7$	415.2116 $[M + H]^+$, 400.1888 $[M + H\text{-}CH_3]^+$, 384.1932 $[M + H\text{-}OCH_3]^+$, 369.1699 $[M + H\text{-}OCH_3\text{-}CH_3]^+$, 338.1520 $[M + H\text{-}2OCH_3\text{-}CH_3]^+$	7-hydroxylated - Schisandrin A	
22	9.9	$[M + H]^+$	449.3111	0.8	$C_{24}H_{32}O_8$	449.3111 $[M + H]^+$, 431.2076 $[M + H\text{-}H_2O]^+$, 382.1767 $[M + H\text{-}H_2O\text{-}2OH\text{-}CH_3]^+$, 373.1656 $[M + H\text{-}2OCH_3\text{-}CH_3]^+$, 358.1428 $[M + H\text{-}2OCH_3\text{-}2CH_3]^+$	7,8-dihydroxy Schisandrin A	
23	10.1	$[M + H]^+$	432.3115	0.9	$C_{23}H_{28}O_8$	432.3115 $[M + H]^+$, 414.3028 $[M + H\text{-}H_2O]^+$, 357.2811 $[M + H\text{-}CH_2O_2\text{-}CH_3]^+$, 339.2707 $[M + H\text{-}CH_2O_2\text{-}CH_3\text{-}H_2O]^+$, 321.2591 $[M + H\text{-}CH_2O_2\text{-}CH_3\text{-}2H_2O]^+$	11-hydroxylated-Schisandrol B	Metabolite of Schisandrol B

In the normal group, the lung tissue was intact with no inflammatory cell infiltration around the airway, and the mucosa was free of proliferation and deformation. Whereas, the rats in the model group occurred inflammatory cellular infiltration, alveolar wall telangiectasia, and bronchial wall thickening (Fig. 2C). Upon treatment, the detrimental effect on the lung caused by allergic asthma was improved, as demonstrated by the remission of the infiltration of pulmonary inflammatory cells in the lung. Besides, when compared with RSC, the ameliorative effect in WSC-H treated groups at the same doses was more prominent in the lung tissues.

Optimization of sample processing method

To determine the optimal serum pretreatment method, a comparison was carried out between the methanol precipitation method and the acetonitrile precipitation method. Based on the results obtained in the positive mode, 23 compounds could be detected in methanol treatment, while only 14 compounds could be detected in acetonitrile treatment (Fig. 3). Although no corresponding compounds were detected in the negative ion mode, by comparing the TIC diagrams of methanol treated serum and acetonitrile treated serum, it can be found that the information in the TIC diagram was more abundant under the methanol treatment method (Fig. 4). Thereupon, the methanol precipitation method was finally selected as the treatment method for serum samples.

Identification of potentially bioactive compounds of WSC

The efficacy comparison experiment carried out in this work has proved that the therapeutic effect on allergic asthma rats of WSC was more potent than RSC, in order to further explore the pharmacodynamic material basis of WSC, we adopted serum pharmacochemistry to screen the ingredients absorbed into the blood of WSC-H.

Specifically, the serum samples were analyzed by comparing the fragment pattern and retention time of the UPLC-Q-TOF-MS/MS data under the positive mode and negative mode (Fig. 5A and Fig. 5B). As a result, a total of 12 components such as Schisandrin, Schisandrol B, Merulinic acid A, Gomisin R, Gomisin D, Schisandrin B, Dimethyl citrate, Neoisostegane, Schisandrin C, Schinsanlignone A, Schisantherin A, and Schisandrin A were identified by comparison with the control sample, of which the first 10 were detected in prototype form and the last 2 were not detected in prototype form. In addition, 13 metabolites were metabolized from the 3 components of Schisantherin A, Schisandrin A, and Schisandrol B through demethylation or hydroxylation, which were consistent with those reported in the literature (Fig. 5C and Table 1). Taking the metabolite of Schisantherin A as an example, the speculated cracking process was illustrated in combination with references, as shown in Fig. 6.

Table 2
Identification of chemical compounds in the decoction of RSC and WSC decoction pieces

No.	RT (min)	Adduction	M/Z	ppm	Formula	Fragments	Identification	Type
1	16.9	$[M + H]^+$	417.2237	-8.1	$C_{24}H_{32}O_6$	417.2234 $[M + H]^+$, 402.2005 $[M + H-CH_3]^+$, 371.1836 $[M + H-CH_3-OCH_3]^+$, 347.1465 $[M + H-C_5H_{10}]^+$, 316.1280 $[M + H-C_5H_{10}-OCH_3]^+$, 301.1048 $[M + H-CH_3-OCH_3-5CH_2]^+$	Schisandrin A*	Lignan
2	17.4	$[M + H]^+$	401.8561	-5.7	$C_{23}H_{28}O_6$	401.1957 $[M + H]^+$, 370.1746 $[M + H-OCH_3]^+$, 331.1149 $[M + H-C_5H_{10}]^+$, 316.0927 $[M + H-CH_3-C_5H_{10}]^+$, 300.0969 $[M + H-CH_3-O-C_5H_{10}]^+$	Schisandrin B*	Lignan
3	15.5	$[M + H]^+$	417.1892	-3.8	$C_{23}H_{28}O_7$	417.1815 $[M + H]^+$, 399.1699 $[M + H-H_2O]^+$, 358.1321 $[M + H-H_2O-CH_3-C_2H_4]^+$, 314.1084 $[M + H-H_2O-CH_3-C_2H_4-CH_3CO]^+$	Schisandrol B*	Lignan
4	15.5	$[M + H]^+$	537.2101	-3.4	$C_{30}H_{32}O_9$	538.1772 $[M + H]^+$, 415.1742 $[M + H-C_6H_5COOH]^+$, 371.1482 $[M + H-C_6H_5COOH-CH_3CHO]^+$, 340.1298 $[M + H-C_6H_5COOH-CH_3CHO-OCH_3]^+$	Schisantherin A*	Lignan
5	17.6	$[M + H]^+$	385.1646	0.1	$C_{22}H_{24}O_6$	385.1650 $[M + H]^+$, 355.1546 $[M + H-OCH_3]^+$, 285.0754 $[M + H-OCH_3-C_5H_{10}]^+$	Schisandrin C*	Lignan

*: Ingredients to be compared with the standards.

No.	RT (min)	Adduction	M/Z	ppm	Formula	Fragments	Identification	Type
6	15.3	$[M + H]^+$	403.2098	-4.3	$C_{23}H_{30}O_6$	403.2080 $[M + H]^+$, 388.1849 $[M + H\text{-}CH_3]^+$, 371.1827 $[M + H\text{-}CH_3\text{-}OH]^+$, 340.1645 $[M + H\text{-}CH_3\text{-}OH\text{-}OCH_3]^+$, 325.1410 $[M + H\text{-}2CH_3\text{-}OH\text{-}OCH_3]^+$	Schisanhenol*	Lignan
7	16.1	$[M + H]^+$	515.2263	-2.4	$C_{28}H_{34}O_9$	515.2228 $[M + H]^+$, 469.2183 $[M + H\text{-}CO\text{-}H_2O]^+$, 385.1615 $[M + H\text{-}CO\text{-}H_2O\text{-}C_5H_8O]^+$, 354.1441 $[M + H\text{-}CO\text{-}H_2O\text{-}C_5H_8O\text{-}OCH_3]^+$	Schisantherin B	Lignan
8	14.8	$[M + H]^+$	431.2033	-5.6	$C_{24}H_{30}O_7$	431.2033 $[M + H]^+$, 400.1865 $[M + H\text{-}OCH_3]^+$, 372.1549 $[M + H\text{-}OCH_3\text{-}C_2H_4]^+$, 356.1598 $[M + H\text{-}OCH_3\text{-}C_2H_4\text{-}O]^+$	Schinsanlignone A	Lignan
9	16.17	$[M + H]^+$	387.1790	-3.2	$C_{22}H_{26}O_6$	387.1786 $[M + H]^+$, 372.1557 $[M + H\text{-}CH_3]^+$, 357.1676 $[M + H\text{-}CH_3\text{-}OH]^+$	Gomisin M_2	Lignan
10	13.1	$[M + H]^+$	389.1940	-4.8	$C_{22}H_{28}O_6$	389.1935 $[M + H]^+$, 357.1678 $[M + H\text{-}OCH_3]^+$, 326.1500 $[M + H\text{-}2OCH_3]^+$	Gomisin J	Lignan
11	13.9	$[M + H]^+$	391.2113	-0.8	$C_{22}H_{30}O_6$	391.2113 $[M + H]^+$, 327.1602 $[M + H\text{-}2OCH_3]^+$, 257.0815 $[M + H\text{-}2OCH_3\text{-}C_7H_6O_2]^+$	Pregomisin	Lignan
12	12.9	$[M + H]^+$	401.1591	-0.9	$C_{22}H_{24}O_7$	401.1602 $[M + H]^+$, 352.1309 $[M + H\text{-}OCH_3]^+$, 337.1058 $[M + H\text{-}OCH_3\text{-}CH_3]^+$	Gomisin R	Lignan

*: Ingredients to be compared with the standards.

No.	RT (min)	Adduction	M/Z	ppm	Formula	Fragments	Identification	Type
13	12.9	$[M+H]^+$	531.2206	-3.5	$C_{28}H_{34}O_{10}$	531.2152 $[M+H]^+$, 485.2161 $[M+H-CH_2O_2]^+$, 401.1588 $[M+H-C_5H_8O]^+$, 383.1488 $[M+H-C_5H_8O-H_2O]^+$	Gomisin D	Lignan
14	15.5	$[M+H]^+$	415.1742	-4.4	$C_{23}H_{26}O_7$	415.1742 $[M+H]^+$, 385.1644 $[M+H-CH_2O]^+$, 371.1481 $[M+H-CH_2O-CH_3]^+$	Neoisostegane	Lignan
15	14.5	$[M+H]^+$	523.6521	-4.0	$C_{30}H_{34}O_8$	523.2287 $[M+H]^+$, 493.1810 $[M+H-2CH_3]^+$, 409.1613 $[M+H-2CH_3-C_6H_5-2H_2O]^+$	Benzoyl-gomisin-H	Lignan
16	17.0	$[M+H]^+$	219.1733	-4.7	$C_{15}H_{22}O$	219.1743 $[M+H]^+$, 201.1632 $[M+H-H_2O]^+$, 175.1465 $[M+H-H_2O-2CH_3]^+$	Chamigrenal	Organic acid
17	17.6	$[M+H]^+$	521.2156	-2.7	$C_{30}H_{32}O_8$	521.2134 $[M+H]^+$, 421.1615 $[M+H-C_5H_8O_2]^+$	Benzoylgomisin O	Lignan
18	12.4	$[M+H]^+$	433.1891	-2.9	$C_{24}H_{32}O_7$	433.1891 $[M+H]^+$, 384.1905 $[M+H-CH_4O_2]^+$, 369.1672 $[M+H-CH_4O_2-CH_3]^+$, 338.1488 $[M+H-CH_4O_2-CH_3-CH_3O]^+$	Schisandrin*	Lignan
19	11.2	$[M+H]^+$	419.2052	-2.9	$C_{23}H_{30}O_7$	419.2062 $[M+H]^+$, 369.1693 $[M+H-CH_3-2OH]^+$, 323.1276 $[M+H-2CH_3-2OH-CO]^+$	Gomisn S/T	Lignan
20	17.6	$[M+H]^+$	537.2463	1.8	$C_{31}H_{36}O_8$	537.2463 $[M+H]^+$, 437.1931 $[M+H-C_5H_8O_2]^+$, 384.1933 $[M+H-C_5H_8O_2-H_2O-OCH_3]^+$	Benzoylgomisin Q	Lignan

*: Ingredients to be compared with the standards.

No.	RT (min)	Adduction	M/Z	ppm	Formula	Fragments	Identification	Type
21	2.4	$[M+H]^+$	221.0655	2.3	$C_8H_{12}O_7$	221.0655 $[M+H]^+$, 157.0484 $[M+H\text{-}OH\text{-}COOCH_3]^+$, 139.0023 $[M+H\text{-}OH\text{-}COOCH_3\text{-}H_2O]^+$	Dimethyl citrate	Organic acid
22	18.9	$[M+H]^+$	471.3459	-2.1	$C_{30}H_{46}O_4$	471.3467 $[M+H]^+$, 453.3241 $[M+H\text{-}H_2O]^+$, 435.3241 $[M+H\text{-}2H_2O]^+$	Nigranoic acid	Organic acid
23	12.0	$[M+H]^+$	531.2594	1.0	$C_{29}H_{38}O_9$	531.2596 $[M+H]^+$, 471.2378 $[M+H\text{-}2CH_2O]^+$, 443.2426 $[M+H\text{-}CO\text{-}2CH_2O]^+$, 425.2342 $[M+H\text{-}CO\text{-}2CH_2O\text{-}H_2O]^+$	Angeloylgomisin Q	Lignan
24	11.1	$[M+H]^+$	499.2328	0.6	$C_{28}H_{34}O_8$	499.2328 $[M+H]^+$, 481.2217 $[M+H\text{-}H_2O]^+$, 463.2100 $[M+H\text{-}2H_2O]^+$, 421.2009 $[M+H\text{-}2H_2O\text{-}C_2H_2O]^+$	Angeloylisogomisin O	Lignan
25	15.2	$[M+H]^+$	235.1722	3.2	$C_{15}H_{22}O_2$	235.1722 $[M+H]^+$, 217.1615 $[M+H\text{-}H_2O]^+$, 199.1513 $[M+H\text{-}2H_2O]^+$	β-chamigrenic acid	Organic acid
26	21.0	$[M+H]^+$	455.3521	6.17	$C_{30}H_{46}O_3$	455.3521 $[M+H]^+$, 437.3411$[M+H\text{-}H_2O]^+$, 419.3304 $[M+H\text{-}2H_2O]^+$, 401.3363 $[M+H\text{-}3H_2O]^+$	Schisandronic acid	Organic acid
27	21.3	$[M+H]^+$	391.3340	-1.0	$C_{24}H_{38}O_4$	391.3340 $[M+H]^+$, 279.1769 $[M+H\text{-}7CH_2\text{-}CH_3+H]^+$	Merulinic acid A	Organic acid
28	1.2	$[M-H]^+$	191.0187	-3.2	$C_6H_8O_7$	191.0187 $[M-H]^+$, 173.0107 $[M-H\text{-}H_2O]^+$, 155.0016 $[M-H\text{-}2H_2O]^+$	Citric acid	Organic acid

*: Ingredients to be compared with the standards.

No.	RT (min)	Adduction	M/Z	ppm	Formula	Fragments	Identification	Type
29	20.1	$[M-H]^+$	456.3606	4.7	$C_{30}H_{48}O_3$	456.3606 $[M-H]^+$, 409.3486 $[M-H-COOH]^+$	Betulinic acidBetulinic acid	Organic acid
30	0.9	$[M-H]^+$	133.0172	1.4	$C_4H_6O_5$	133.0172 $[M-H]^+$, 115.0065 $[M-H-H_2O]^+$, 114.6473 $[M-H-H_2O-H]^+$	Malic acid	Organic acid
31	1.1	$[M-H]^+$	173.0093	0.8	$C_7H_{10}O_5$	173.0093 $[M-H]^+$, 129.0220 $[M-H-2H_2O-COOH]^+$ 111.0105 $[M-H-3H_2O-COOH]^+$	Shikimic acid	Organic acid
32	4.3	$[M-H]^+$	291.0876	4.4	$C_{15}H_{14}O_6$	291.0860 $[M-H]^+$, 207.0649 $[M-H-5OH]^+$, 189.0554 $[M-H-5OH-H_2O]^+$, 161.0601 $[M-H-6OH-H_2O]^+$	Catechin	Organic acid
*: Ingredients to be compared with the standards.								

There were some molecular ions at m/z 415.1751 $[M + H-H_2O]^+$, m/z 384.1572 $[M + H-H_2O-OCH_3]^+$, m/z 369.1326 $[M + H-H_2O-OCH_3-CH_3]^+$, m/z 345.1315 $[M + H-H_2O-C_5H_{10}]^+$, m/z 301.1074 $[M + H-H_2O-CO_2-C_5H_{10}]^+$ and m/z 286.0847 $[M + H-H_2O-CO_2-C_5H_{10}-CH_3]^+$ that were aligned with the fragmentation pattern of m/z 433.185. Based on the above results, compound 11 could be identified as 6-debenzoyl-Schisantherin A.

The formula of compound 12 was confirmed to be $C_{22}H_{26}O_8$ which was only 14 Da lower than that of Schisantherin A. The fragments of m/z 401.1632 $[M + H-H_2O]^+$, m/z 369.1361 $[M + H-H_2O-CH_3OH]^+$, m/z 331.1193 $[M + H-H_2O-C_5H_{10}]^+$, and m/z 316.0941 $[M + H-H_2O-C_5H_{10}-CH_3]^+$were detected. Thus, it was confirmed that compound 12 was 3-demethylation-6-debenzoyl-Schisantherin A.

Compound 13 and compound 14 were detected at 15.5 min and its $[M + H]^+$ ion at m/z 415.1760 was 18 Da lower than that of Schisantherin A. The spectrum showed ions at m/z 397.1634 $[M + H-H_2O]^+$, m/z 385.1650 $[M + H-OCH_2]^+$, m/z 371.1489 $[M + H-OCH_2-CH_3]^+$, m/z 342.1110 $[M + H-OCH_2-CH_3-HCO]^+$, and m/z 340.1316 $[M + H-OCH_2-CH_2-OCH_3]^+$, which were aligned with Schisantherin A. Hence, compound 13 and compound 14 were identified as 7,8-dehydration-6-debenzoyl-Schisantherin A and 7,17-dehydration-6-debenzoyl-Schisantherin A, respectively [28]. The secondary mass spectra of the above compounds were displayed in Fig. 6.

Identification of chemical compounds in RSC and WSC decoction pieces

As was shown in Fig. 7A and Fig. 7B, the decoction of RSC and WSC were analyzed using positive and negative modes under optimal conditions. Based on the retention time, fragmentation pattern, precise mass measurements, and relative literature, we identified a total of 32 compounds originating from the decoction of RSC and WSC, including 21 lignans and 11 organic acids. Concrete information of each compound was shown in Table 2.

The lignans in RSC are mostly biphenyl cyclooctene lignans, which can be divided into three types according to the differences of carbon substituents at positions 2, 3, 6, 7, 12, 13, and 14. The first is that there is no substituent on the carbon at positions 6 and 7, such as Schisandrin B; The second is hydroxyl substitution at position 7 and no substituent at position 6, such as Schisandrin B; The third is hydroxyl substitution at position 7 and acyloxy substitution at position 6, such as Schisantherin A. The final data obtained by mass spectrometry showed that lignans had a high response value in positive mode. During the analysis of chemical components, it was found that most of the excimer ion peaks of these compounds were $[M + Na]^+$, $[M + NH_4]^+$, or $[M + H]^+$ peaks.

The fragmentation pattern of the above three types of lignans is summarized: (1) Lignans without substituents at positions 6 and 7 are inclined to lose methyl or methoxy, resulting in the fracture of octatomic ring and the loss of C_5H_{10}, or the ring broke and loss C_5H_{10}, and then demethylates or methoxy groups to form new ion fragments. (2) Lignans with hydroxyl substitution at position 7 and no substituent at position 6 are generally dehydrated first, and most of them are cleaved in the source, and then demethylated or methoxy to obtain fragment ions. Or after dehydration, the biphenyl ring breaks, C_3H_6 and C_4H_8 are lost, and new fragments are obtained. (3) Lignans with hydroxyl substitution at position 7 and acyloxy substitution at position 6 are easy to remove RCOOH at position 6, followed by dehydration or CH_3CHO group at position 7. In this experiment, Schisandrin A, Schisandrin B, Schisandrol B, and Schisantherin A were taken as examples to enumerate the analytical process in detail.

Compound 1, with a retention time of 16.9 min, and molecular formula of $C_{24}H_{32}O_6$, exhibited fragment ions at m/z 417.2234 $[M + H]^+$, m/z 402.2005 $[M + H\text{-}CH_3]^+$, m/z 371.1836 $[M + H\text{-}CH_3\text{-}OCH_3]^+$, m/z 347.1465 $[M + H\text{-}C_5H_{10}]^+$, m/z 316.1280 $[M + H\text{-}C_5H_{10}\text{-}OCH_3]^+$, and m/z 301.1048 $[M + H\text{-}CH_3\text{-}OCH_3\text{-}5CH_2]^+$ in positive ion mode. Based on the fragments of (15 Da) CH_3, (31 Da) OCH_3, (70 Da) C_5H_{10}, and (31 Da) OCH_3, it could be preliminarily judged that compound 1 was Schisandrin A [29]. The fragmentation pathway was consistent with those in the literature. The possible cleavage fragmentation pathway of Schisandrin A was shown in Fig. 7C.

Compound 2 had a retention time of 17.4 min, molecular formula of $C_{23}H_{28}O_6$ and showed fragment ions at m/z 401.8561 $[M + H]^+$, m/z 386.1691 $[M + H\text{-}CH_3]^+$, m/z 370.1745 $[M + H\text{-}OCH_3]^+$, m/z 331.1149 $[M + H\text{-}C_5H_{10}]^+$, m/z 316.0927 $[M + H\text{-}CH_3\text{-}C_5H_{10}]^+$, m/z 300.0969 $[M + H\text{-}CH_3\text{-}O\text{-}C_5H_{10}]^+$, and m/z 285.1080 $[M + H\text{-}CH_3\text{-}C_5H_{10}\text{-}O\text{-}CH_3]^+$ in positive mode. Pursuant to the fragment and the literature [30], the compound could be identified as Schisandrin B. The specific possible fragmentation process was shown in Fig. 7D.

Taking compound 3 as an example, according to its retention time of 15.4 min and m/z 417.1909, it was speculated that it might be Schisandrol B ($C_{23}H_{28}O_7$). There were four characteristic fragments on the map, including m/z 399.1699, m/z 357.1345, m/z 314.1084, and m/z 285.0758. Among them, the m/z 399.1699 $[M + H\text{-}H_2O]^+$ ion fragment lost CH_3 and C_2H_4 to form m/z 357.1345 $[M + H\text{-}H_2O\text{-}CH_3\text{-}C_2H_4]^+$ ion fragment, then lost CH_3CO group to produce m/z 314.1084 $[M + H\text{-}H_2O\text{-}CH_2\text{-}C_2H_4\text{-}CH_3\text{-}CO]^+$ ion fragment, and finally lost methoxy group to produce m/z 285.0758 $[M + H\text{-}H_2O\text{-}CH_2\text{-}C_2H_4\text{-}CH_3\text{-}CO\text{-}OCH_3]^+$ ion fragment. Hence, it was determined as Schisandrol B [31]. Its cleavage law and mass spectrum were shown in Fig. 7E.

Compound 4 showed a retention time of 15.4 min and the molecular formula of $C_{30}H_{32}O_9$. Four fragments at m/z 538.1772 $[M + H]^+$, m/z 415.1742 $[M + H\text{-}C_6H_5COOH]^+$, m/z 371.1482 $[M + H\text{-}C_6H_5COOH\text{-}CH_3CHO]^+$, and m/z 340.1298 $[M + H\text{-}C_6H_5COOH\text{-}CH_3CHO\text{-}OCH_3]^+$ were detected in positive mode. Compound 4 could be determined as Schisantherin A through comparison with the reference and literature [32]. The possible fragmentation patterns of Schisantherin A were presented in Fig. 7F.

Analysis of differential chemical constituents between RSC and WSC decoction pieces

Considering that wine steaming will affect the chemical composition of medicinal materials and thus lead to changes in drug efficacy, the changes of chemical components between the decoction of WSC and RSC were analyzed by UPLC-Q-TOF-MS/MS to further elaborate on the possible Q-markers for the efficacy of WSC.

The results demonstrated that all of them were distinguished from each other (Fig. 8A and Fig. 8B). In the loading plot, the X-axis represents the first principal component and the Y-axis represents the second principal component (Fig. 8C and Fig. 8D). The greater their absolute value, the more significant the difference between the compounds. Under the above method, 12 compounds with varying dissolution rates were identified (Fig. 8E and Fig. 9). Specifically, the dissolution rates of Schisandrin A, Schisandrin B, Schisanhenol, Gomisin D, Schisandrol B, and Schisandrin displayed an upward trend, while the dissolution rates of Schisantherin B, Citric acid, Malic acid, Nigranoic acid, Catechin, and Schisantherin A revealed an opposite trend after wine-steam processing.

Combined with the potential pharmacodynamic active components of WSC, we speculated that the improvement of the efficacy of WSC might be related to the increase of the dissolution rates of Schisandrin, Schisandrol B, Schisandrin A, Schisandrin B, and Gomisin D. Therefore, we preliminary selected Schisandrin, Schisandrol B, Schisandrin A, Schisandrin B, and Gomisin D as Q-markers that reflecting the efficacy of WSC.

In vivo efficacy validation

MTC measurement results

As illustrated in Fig. 10, the dosage was determined according to the MTC of each component. Finally, the MTC of Schisandrin, Schisandrol B, Schisandrin A, Schisandrin B, and Gomisin D were determined to be 160μM, 80 μM, 20μM, 10μM, and 10μM, respectively.

Screening of administration time points

ELISA assay showed that TNF-α and IL-6 expression in the 1h and 2h groups were elevated and the expression of IL-10 was decreased compared with the control group (Fig. 11A). In addition, the expression of indicators was more obvious in the 2h group ($P < 0.01$). However, no obvious difference in the levels of TNF-α, IL-6, and IL-10 was observed among the 4h, 6h, and normal groups. Therefore, 2h after tail amputation was finally selected as the deadline for administration.

Efficacy comparison results

As shown in Fig. 11B, compared with the normal group, the expression of TNF-α and IL-6 in the model group was prominently elevated ($P < 0.01$), and the content of IL-10 was conspicuously reduced ($P < 0.01$), proving that the zebrafish inflammation model was successfully established, and the research results based on this model had high credibility. However, treatment with all monomer components significantly reduced the production of TNF-α and IL-6 caused by tail amputation but increased the expression of IL-10 ($P < 0.01$), Interestingly, all five components exerted the anti-inflammatory effects in a dose-dependent manner, i.e. the higher the administered dose, the stronger the efficacy in TNF-α, IL-6, and IL-10. These results suggested that Schisandrin, Schisandrol B, Schisandrin A, Schisandrin B, and Gomisin D caused an anti-inflammatory effect, combined with previous reports that RSC can treat asthma by anti-inflammatory [21], implying the improvement of the efficacy of WSC was related to the 5 Q-markers.

Discussion

RSC is the core prescribed herbs frequently used by ancient and modern doctors to treat asthma [33]. In the Synopsis of the Golden Chamber published in the Han Dynasty, RSC was commonly applied in the prescriptions of warming the lung to dissipate phlegm with the function of restraining lung Qi and relieving cough [34], such as Xiaoqinglong decoction [35] and Sheganmahuang decoction [36]. In clinical application, steaming with wine is often used to achieve the purpose of enhancing efficiency. As one of the commonly used adjuvants in processing, yellow rice wine can promote drug blood circulation and accelerate the release of effective components [37]. However, the Q-markers related to the efficacy of the WSC decoction pieces are still unclear, and the exclusive quality standard of WSC has not been established.

OVA is frequently used in asthma modeling and can cause significant allergic airway inflammation [38]. In this study, allergic asthma model was established by mainly OVA stimulation, supplemented by aluminum hydroxide. It was found that the rats in the model group appeared resemble asthma symptoms like shortness of breath, wheezing, and sneezing. Considering that asthma is marked by lung inflammation, which is also a typical feature of asthma, the pathological status of the lungs were evaluated [39]. In the model group, we observed marked inflammatory infiltration in the lungs with thickening of the bronchial wall (Fig. 2C). These results were in accordance with previously reported studies[40–41], suggested that pathological changes occurred in the tissues corresponding to asthma in the model group. In order to further visually reflect the establishment of the model, we investigated the expression of IgE, IFN-γ and IL-4 in the model group. The results showed that the level of IFN-γ decreased and the level of IL-4 and IgE increased in the model group. Among them, the overexpression of Th_2 cytokines such as IL-4 and the decrease of Th_1 cytokines such as IFN-γ are the main manifestations of Th1/Th2 imbalance, which is also the key mechanism of mediating asthma attack [42, 43]. Therefore, it is speculated that the model group has Th1/Th2 imbalance. In addition, the increase of IgE and other inflammatory factors is also one of the important causes in the development of asthma [44]. Combined with the inflammatory infiltration phenomenon observed in the lungs, the successful establishment of allergic asthma model has been confirmed, and can be used to compare the efficacy of RSC and WSC. Efficacy studies showed that both RSC and WSC induced an increase in IFN-γ levels, a decrease in IL-4 and IgE levels, and improved lung inflammation ((Fig. 2B and Fig. 2C)), suggesting that they could play a role in the treatment of asthma by regulating the imbalance of Th1/Th2 ratio and reducing IgE levels. In addition, the regulatory effect of WSC was better than that of RSC at the same dose, and the effect was more obvious in the high-dose group. Considering allergic asthma model established in this paper is a classic model of high credibility and the dosage of RSC and WSC complies with clinical requirements, it is speculated that the outcomes obtained in this paper have a certain reference value for clinical practice, and provide data support for the application of WSC in the clinical treatment of asthma.

The above results have shown that the anti-asthma effect of WSC is better than that of RSC, which has research and application value. In order to further explore the chemical components of WSC, serum pharmacochemistry, a method based on the theory that "the components absorbed and metabolized in blood are the potential active components", were used to investigate the bioactive components of WSC [45, 46]. Our results demonstrated that they were all prototype components or metabolic components of lignans (consisting of 10 prototypes and 13 metabolites) (Table 1 and Fig. 5).

Although the quality evaluation standard of RSC with Schisandrin A as the index has been included in Chinese Pharmacopoeia, there are few studies on WSC, and its exclusive quality standard evaluation method has not been established. At present, our study manifested that WSC exhibited more excellent efficacy. In order to distinguish the quality inspection methods of RSC and WSC from the evaluation components, UPLC-Q-TOF-MS/MS was used to identify the common and differential chemical components between the WSC and RSC decoction pieces to screen the exclusive Q-markers of WSC. The results demonstrated that there were 32 common components between RSC and WSC decoction pieces, of which the dissolution rates of 12 components were different after being processed (Table 2, Fig. 7, and Fig. 8). Combined with the analysis results of components absorbed into the blood of WSC-H group, it was found that 5 components, such as Schisandrin, Schisandrol B, Schisandrin A, Schisandrin B, and Gomisin D, have higher dissolution rates than RSC after steaming with wine, suggesting the reasons for the superior efficacy. Therefore, we preliminarily screened these 5 components as Q-markers related to the WSC efficacy.

Asthma is a chronic inflammatory disorder of the airways in which many inflammatory mediators, cytokines, and adhesion molecules play a role [47]. Higher secretion of Th2-type cytokines, such as IL-4, IL-5, and IL-13 in the allergic airway, resulting in larger amounts of recruitment of inflammatory cells and airway hyperresponsiveness [48], which can be concluded that asthma severity could be responsible for airway inflammation. Therefore, we examined the efficacy of 5 components from an anti-inflammatory point of view. As a result, the zebrafish inflammation model was successfully established, as demonstrated by the elevated TNF-α and IL-6 and the reduction of IL-10 (Fig. 10A) [49]. In addition, all 5 components exerted the anti-inflammatory effects in a dose-dependent manner, combined with previous reports that RSC and WSC can treat asthma by anti-inflammatory(Fig. 10B) [21], implying that Schisandrol A, Schisandrol B, Schisandrin A, Schisandrin B, and Gomisin D was Q-markers reflecting the efficacy of the decoction pieces.

Conclusion

In this study, Q-markers related to WSC efficacy were screened by pharmacodynamic comparison-component screening-component validation in vivo efficacy. Taking allergic asthma rats as a model, the efficacy of the decoction pieces of WSC was better than that of RSC at the same dose based on the pharmacodynamic comparison. 12 components of WSC have been detected in blood, among which 5 components, Schisandrin, Schisandrol B, Schisandrin A, Schisandrin B, and Gomisin D, have increased dissolution in water decoction after steaming with wine. In vivo efficacy verification showed that these 5 components were effective, namely Q-markers reflecting the superior efficacy of WSC decoction pieces. This study provides theoretical support for the establishment of WSC decoction piece exclusive quality evaluation standards.

Abbreviations

TCM: Traditional Chinese medicine; WSC: Wine-steamed Schisandra Chinensis Fructus; RSC: Raw Schisandra Chinensis Fructus; UPLC-Q-TOF-MS/MS: Ultra-performance liquid chromatography quadrupole time-of-flight mass spectrometry; Quality markers: Q-markers; Dex: Dexamethasone; IgE: Immunoglobulin E; IFN-γ: Interferon γ; IL-4: Interleukin 4; HE: Hematoxylin-eosin; PCA: Principal component analysis; MTC: Maximum tolerance concentration; TNF-α: Tumor necrosis factor-α; IL-6: Interleukin 6; IL-10: Interleukin 10

Declarations

Author contributions statement

Zhongyuan Qu: Writing - Review & Editing, Funding acquisition. Yifan Bing: Writing - review & editing, Data curation. Tianlei Zhang: Visualization. Yan Zheng: Data curation. Shuang Wu: Investigation. Chenfeng Ji: Methodology. Wenlan Li: Methodology. Xiang Zou: Conceptualization, Supervision.

Funding

The study was supported by the Key Research and Development Guidance Project of Heilongjiang Province (GZ20210110); Heilongjiang Natural Science Foundation Joint Guidance Project (LH2022H001); Applied Technology Research and Development program of Heilongjiang Province(GA19C107); Harbin University of Commerce Youth Innovation Talent Support Program(2020CX11); Postdoctoral Research Fund of Heilongjiang Province (LBH-Q16133).

Availability of data and materials

The datasets used and/or analyzed during the current study are available from the corresponding author on reasonable request.

Ethics approval and consent to participate

This research was conducted under approval and guidance of the Animal Ethics Committee of the School of Pharmacy, Harbin University of Commerce (HSDYXY2018025).

Consent for publication

All authors agree to publish this article.

Competing interests

All authors declare that there are no conficts of interest.

References

1. Corren J. Asthma phenotypes and endotypes: an evolving paradigm for classification. Discov Med. 2013;15:243-249.
2. Ellwood P, Asher MI, Billo NE, et al. The Global Asthma Network rationale and methods for Phase I global surveillance: prevalence, severity, management and risk factors. Eur Respir J. 2017;49:1601605. https://doi.org/10.1183/13993003.01605-2016.
3. Global Burden of Disease Study 2013 Collaborators. Global, regional, and national incidence, prevalence, and years lived with disability for 301 acute and chronic diseases and injuries in 188 countries, 1990-2013: a systematic analysis for the Global Burden of Disease Study 2013. Lancet. 2015;386:743-800. https://doi.org/10.1016/S0140-6736(15)60692-4.
4. Akinbami LJ, Moorman JE, Bailey C, et al. Trends in asthma prevalence, health care use, and mortality in the United States, 2001-2010. NCHS Data Brief. 2012;94:1-8.
5. Klimek L, Sperl A, Becker S, Mösges R, Tomazic PV. Current therapeutical strategies for allergic rhinitis. Expert Opin Pharmacother. 2019;20:83-89. https://doi.org/10.1080/14656566.17018.1543401.
6. Nowak A, Zakłos-Szyda M, Błasiak J, Nowak A, Zhang Z, Zhang B. Potential of Schisandra chinensis (Turcz.) Baill. in Human Health and Nutrition: A Review of Current Knowledge and Therapeutic Perspectives. Nutrients. 2019;11:333. https://doi.org/10.3390/nu11020333.
7. Szopa A, Ekiert R, Ekiert H. Current knowledge of Schisandra chinensis (Turcz.) Baill. (Chinese magnolia vine) as a medicinal plant species: a review on the bioactive components, pharmacological properties, analytical and biotechnological studies. Phytochem Rev. 2017;16:195-218. https://doi.org/10.1007/s11101-016-9470-4.
8. Lv X, Xu Z, Xu G, et al. Investigation of the active components and mechanisms of Schisandra chinensis in the treatment of asthma based on a network pharmacology approach and experimental validation. Food Funct. 2020;11:3032-3042. https://doi.org/10.1039/d0fo00087f.
9. Yu W, Ma M, Chen X, et al. Traditional Chinese Medicine and Constitutional Medicine in China, Japan and Korea: A Comparative Study. Am J Chin Med. 2017;45:1-12. https://doi.org/10.1142/S0192415X1750001X.
10. Zhang YC, Sun QB, Yang FD. Zhonghua Yi Shi Za Zhi. 2006;36:72-74.
11. Hancke JL, Burgos RA, Ahumada F. Schisandra chinensis (Turcz.) Baill, Fitoterapia. 1999;70: 451-471, https://doi.org/10.1016/S0367-326X(99)00102-1.
12. Szopa A, Ekiert H. In vitro cultures of Schisandra chinensis (Turcz.) Baill. (Chinese magnolia vine)--a potential biotechnological rich source of therapeutically important phenolic acids. Appl Biochem Biotechnol. 2012;166:1941-1948. https://doi.org/10.1007/s12010-012-9622-y.

13. Li Z, He X, Liu F, Wang J, Feng J. A review of polysaccharides from Schisandra chinensis and Schisandra sphenanthera: Properties, functions and applications. Carbohydr Polym. 2018;184:178-190. https://doi.org/10.1016/j.carbpol.2017.12.058.
14. Gao Y, Wu S. Comprehensive analysis of the phospholipids and phytosterols in Schisandra chinensis oil by UPLC-Q/TOF- MSE. Chem Phys Lipids. 2019;221:15-23. https://doi.org/10.1016/j.chemphyslip.2019.03.003.
15. Zhu H, Zhang L, Wang G, et al. Sedative and hypnotic effects of supercritical carbon dioxide fluid extraction from Schisandra chinensis in mice. J Food Drug Anal. 2016;24:831-838. https://doi.org/10.1016/j.jfda.2016.05.005.
16. Huang P, Tan S, Zhang YX, et al. The effects of wine-processing on ascending and descending: The distribution of flavonoids in rat tissues after oral administration of crude and wine-processed Radix scutellariae. J Ethnopharmacol. 2014;155:649-664. https://doi.org/10.1016/j.jep.2014.05.063.
17. Zhou L, Xu JD, Zhou SS, et al. Integrating targeted glycomics and untargeted metabolomics to investigate the processing chemistry of herbal medicines, a case study on Rehmanniae Radix. J Chromatogr A. 2016;1472:74-87. https://doi.org/10.1016/j.chroma.2016.10.043.
18. Zhao Z, Liang Z, Chan K, et al. A unique issue in the standardization of Chinese materia medica: processing. Planta Med. 2010;76:1975-1986. https://doi.org/10.1055/s-0030-1250522.
19. Chen Z, Ye SY, Zhu RG. The extraordinary transformation of traditional Chinese medicine: processing with liquid excipients. Pharm Biol. 2020;58:561-573. https://doi.org/10.1080/13880209.2020.1778740.
20. Song Y, Shan B, Zeng S, et al. Raw and wine processed Schisandra chinensis attenuate anxiety like behavior via modulating gut microbiota and lipid metabolism pathway. J Ethnopharmacol. 2021;266:113426. https://doi.org/10.1016/j.jep.2020.113426.
21. Li B, Xiao Q, Liu J, et al. Chemical Characterization and Potential Mechanism of the Anti-Asthmatic Activity of a Subfraction from Schisandra chinensis Fruit Extract. J Agric Food Chem. 2022;70:5015-5025. https://doi.org/10.1021/acs.jafc.2c01034.
22. Hu G, Qi Z, Wang A, Jia J. Effects of Deacidification on Composition of Schisandra chinensis Ethanolic Extract and Studies on Acute Toxicity in Mice. Molecules. 2020;25:6038. https://doi.org/10.3390/molecules25246038.
23. M. Westerfleld, M, The Zebrafish Book, Eugene: University of Ore-gon Press. 1995.
24. Wang J, Gao S, Zhang J, Li C, Li H, Lin J. Interleukin-22 attenuates allergic airway inflammation in ovalbumin-induced asthma mouse model. BMC Pulm Med. 2021;21:385. https://doi.org/10.1186/s12890-021-01698-x
25. Shao JZ, Zhang J, Guo XL, Tong XL. Exploration about the Clinical Application and Dosage of Schisandra chinensis, Jilin J Tradit Chin Med. 2019;39: 62-164+168, https://doi.org/10.13463/j.cnki.jlzyy.2019.02.007.
26. Sun M , He M , Korthout H , et al. Characterization of ginsenoside extracts by delayed luminescence, high-performance liquid chromatography, and bioactivity tests. Photochem Photobiol Sci. 2019;18:1138-1146. https://doi.org/10.1039/c8pp00533h.
27. Yin H, Wang J, Wu M, Ma Y, Wang S, Su Q. Preventive Effects of Evodiamine on Dexamethasone-Induced Osteoporosis in Zebrafish. Biomed Res Int. 2019;2019:5859641. https://doi.org/10.1155/2019/5859641.
28. Feng W, Zhou LY, Mu RF, et al. Screening and Identification of the Main Metabolites of Schisantherin a In Vivo and In Vitro by Using UHPLC-Q-TOF-MS/MS. Molecules. 2020;25:258. https://doi.org/10.3390/molecules25020258.
29. Yang S, Shan L, Luo H, Sheng X, Du J, Li Y. Rapid Classification and Identification of Chemical Components of Schisandra Chinensis by UPLC-Q-TOF/MS Combined with Data Post-Processing. Molecules. 2017;22:1778. https://doi.org/10.3390/molecules22101778.
30. Zhou Y, Huang SX, Pu JX, et al. Ultra performance liquid chromatography coupled with quadrupole time-of-flight mass spectrometric procedure for qualitative and quantitative analyses of nortriterpenoids and lignans in the genus Schisandra. J Pharm Biomed Anal. 2011;56:916-927. https://doi.org/10.1016/j.jpba.2011.07.045.

31. Huang X, Song F, Liu Z, Liu S. Studies on lignan constituents from Schisandra chinensis (Turcz.) Baill. fruits using high-performance liquid chromatography/electrospray ionization multiple-stage tandem mass spectrometry. J Mass Spectrom. 2007;42:1148-1161.https://doi.org/10.1002/jms.1246.
32. Shi P, He Q, Zhang Y, Qu H, Cheng Y. Characterisation and identification of isomeric dibenzocyclooctadiene lignans from Schisandra Chinensis by high-performance liquid chromatography combined with electrospray ionisation tandem mass spectrometry. Phytochem Anal. 2009;20:197-206. https://doi.org/10.1002/pca.1115.
33. Lin CC, Xu ZY, Wang BH, et al. Relaxation Effect of Schisandra Chinensis Lignans on the Isolated Tracheal Smooth Muscle in Rats and Its Mechanism. J Med Food. 2021;24:825-832. https://doi.org/ https://doi.org/10.1089/jmf.2021.K.0037.
34. Cheng Z, Song H, Yang Y, Zhou H, Liu Y, Liu Z. Smashing Tissue Extraction of Five Lignans From the Fruit of Schisandra chinensis. J Chromatogr Sci. 2016;54:246-256. https://doi.org/10.1093/chromsci/bmv116.
35. Chen X, Huang Y, Feng J, Jiang XF, Xiao WF, Chen XX. Antioxidant and anti-inflammatory effects of Schisandra and Paeonia extracts in the treatment of asthma. Exp Ther Med. 2014;8:1479-1483. https://doi.org/10.3892/etm.2014.1948.
36. Lin CC, Wang YY, Chen SM, et al. Shegan-Mahuang Decoction ameliorates asthmatic airway hyperresponsiveness by downregulating Th2/Th17 cells but upregulating CD4+FoxP3+ Tregs. J Ethnopharmacol. 2020;253:112656. https://doi.org/10.1016/j.jep.2020.112656.
37. Chen Z, Ye SY, Zhu RG. The extraordinary transformation of traditional Chinese medicine: processing with liquid excipients. Pharm Biol. 2020;58(1):561-573. https://doi.org/10.1080/13880209.2020.1778740.
38. Daubeuf F, Frossard N. Acute Asthma Models to Ovalbumin in the Mouse. Curr Protoc Mouse Biol. 2013;3:31-37. https://doi.org/10.1002/9780470942390.mo120202.
39. Pan LY, Han YQ, Wang YZ, Chen QQ, Wu Y, Sun Y. Mechanism of Yanghe Pingchuan granules treatment for airway remodeling in asthma. Drug Des Devel Ther. 2018;12:1941-1951. https://doi.org/10.2147/DDDT.S159428.
40. Xie Z, Sun H, Li X, Sun W, Yin J. Alteration of lung tissues proteins in birch pollen induced asthma mice before and after SCIT. PLoS One. 2021;16:e0258051. https://doi.org/10.1371/journal.pone.0258051.
41. Piao CH, Bui TT, Fan YJ, et al. In vivo and in vitro anti-allergic and anti-inflammatory effects of Dryopteris crassirhizoma through the modulation of the NF-κB signaling pathway in an ovalbumin-induced allergic asthma mouse model. Mol Med Rep. 2020;22:3597-3606. https://doi.org/10.3892/mmr.2020.11460.
42. Mfengu MOM, Shauli M, Engwa GA, Musarurwa HT, Sewani-Rusike CR. Lippia javanica (Zumbani) herbal tea infusion attenuates allergic airway inflammation via inhibition of Th2 cell activation and suppression of oxidative stress. BMC Complement Med Ther. 2021;21:192. https://doi.org/10.1186/s12906-021-03361-8.
43. Fang L, Yan Y, Xu Z, et al. Tectochrysin ameliorates murine allergic airway inflammation by suppressing Th2 response and oxidative stress. Eur J Pharmacol. 2021;902:174100. https://doi.org/10.1016/j.ejphar.2021.174100.
44. Chiu MH, Hou TY, Fan CK, et al. Catalpol exerts antiallergic effects in IgE/ovalbumin-activated mast cells and a murine model of ovalbumin-induced allergic asthma. Int Immunopharmacol. 2021;96:107782. https://doi.org/10.1016/j.intimp.2021.107782.
45. Wu X, Tang S, Jin Y, et al. Determination of the metabolic profile of gentianine after oral administration to rats by high performance liquid chromatography/electrospray ionization-trap mass spectrometry. J Chromatogr B Analyt Technol Biomed Life Sci. 2015;989:98-103. https://doi.org/10.1016/j.jchromb.2015.01.007.
46. Li J, Bai Y, Bai Y, et al. Pharmacokinetics of Caffeic Acid, Ferulic Acid, Formononetin, Cryptotanshinone, and Tanshinone IIA after Oral Administration of Naoxintong Capsule in Rat by HPLC-MS/MS. Evid Based Complement Alternat Med. 2017;2017:9057238. https://doi.org/10.1155/2017/9057238.
47. Poivre M, Duez P. Biological activity and toxicity of the Chinese herb Magnolia officinalis Rehder & E. Wilson (Houpo) and its constituents. J Zhejiang Univ Sci B. 2017;18:194-214. https://doi.org/10.1631/jzus.B1600299.

48. Zhao ST, Wang CZ. Regulatory T cells and asthma. J Zhejiang Univ Sci B. 2018;19:663-673. https://doi.org/10.1631/jzus.B1700346.
49. Lipworth B, Chan R, Kuo C. Systemic IL-6 and Severe Asthma. Am J Respir Crit Care Med. 2020;202:1324-1325. https://doi.org/10.1164/rccm.202006-2354LE.

Figures

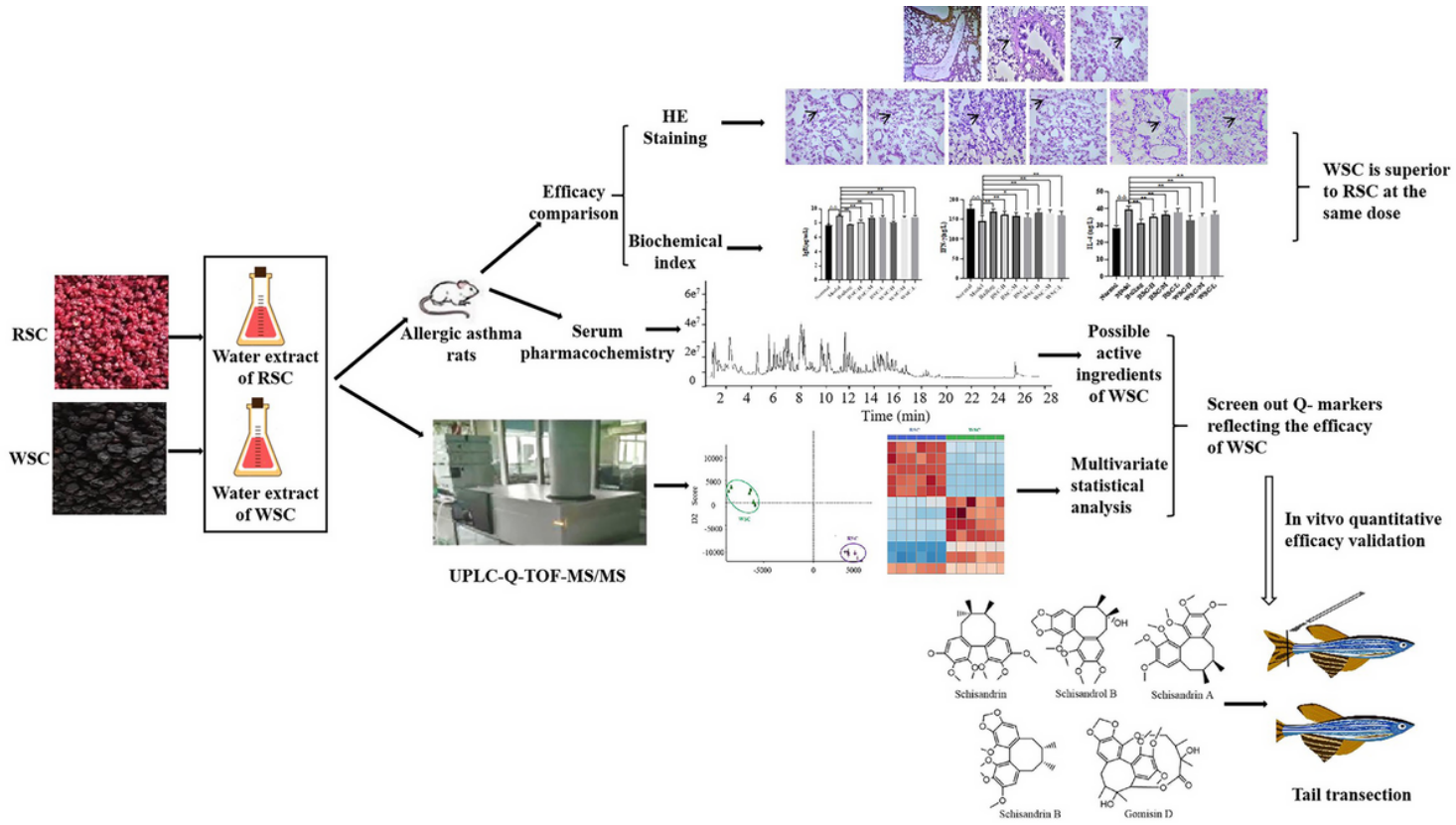

Figure 1

The graphic abstract of the whole study.

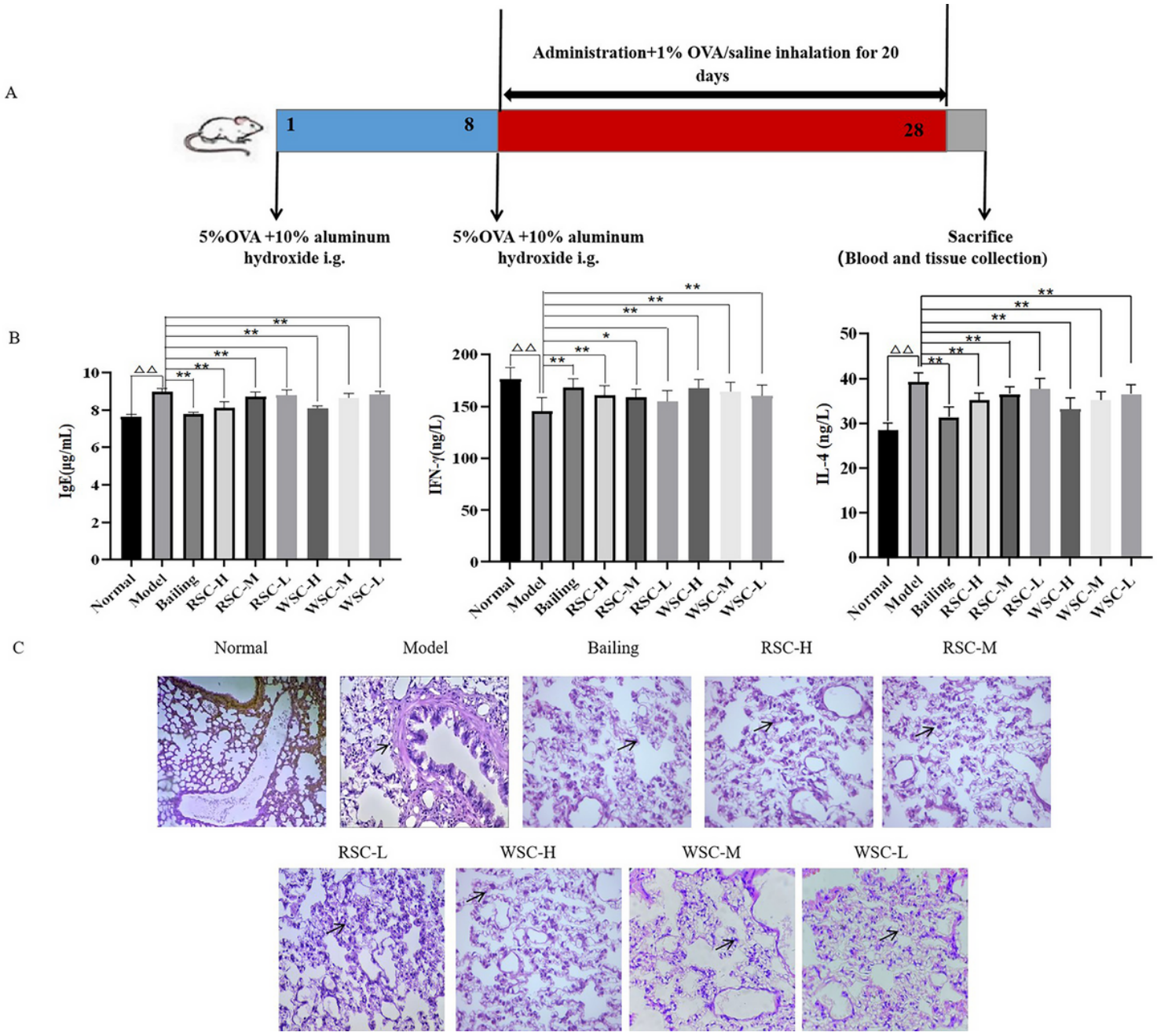

Figure 2

Amelioration effects of RSC and WSC on allergic asthma rats. **A** Establishment of allergic asthma model. **B** Effects of the decoction of RSC and WSC treatment groups on biochemical indexes related to allergic asthma. The data are expressed as mean±SD (n=10). Normal, normal group; Model, model group; Bailing, positive drug group; RSC-H, RSC high-dose group; RSC-M, RSC medium-dose group; RSC-L: RSC low-dose group; WSC-H, WSC high-dose group; WSC-M, WSC medium-dose group; WSC-L, WSC low-dose group. $^{\triangle}p < 0.05$ and $^{\triangle\triangle}p < 0.01$ vs. normal group, $^{*}p < 0.05$ and $^{**}p < 0.01$ vs. model group. **C** Effects of RSC and WSC decoction on lung histomorphology(H&E ×400).

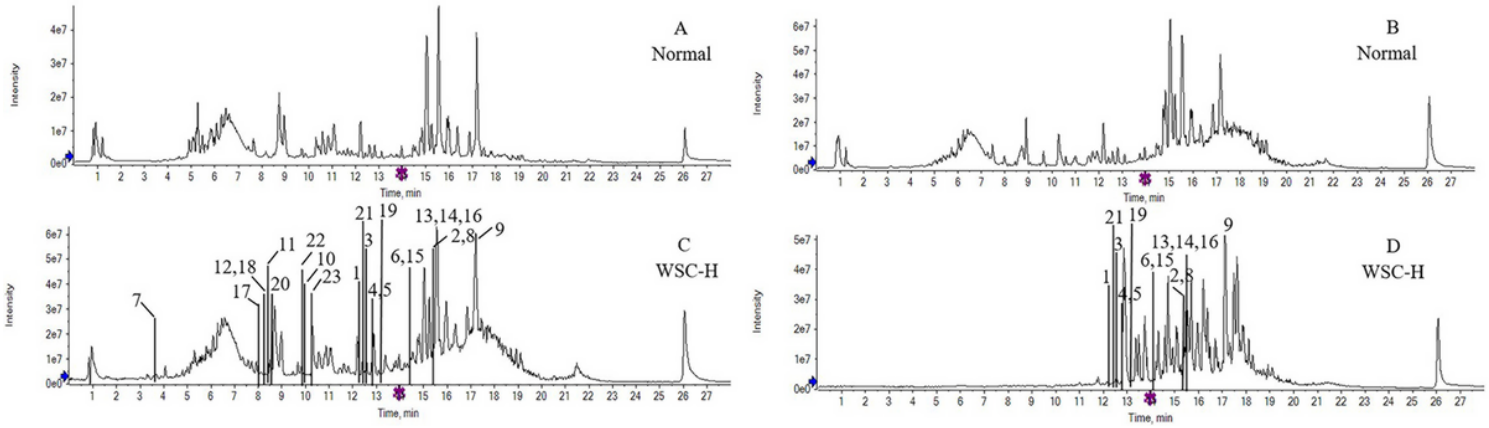

Figure 3

Total ion chromatography (TIC) of normal and WSC serum samples obtained in positive mode after treatment with methanol and acetonitrile, respectively. **A** Total ion chromatography (TIC) of the serum samples in the normal group obtained in positive ion mode after treatment with methanol. **B** TIC of the serum samples in the normal group obtained in positive ion mode after treatment with acetonitrile. **C** TIC of the serum samples in the WSC-H group obtained in positive ion mode after treatment with methanol. **D** TIC of the serum samples in the WSC-H group obtained in positive ion mode after treatment with acetonitrile. Refer to the text for detailed analysis conditions, and the compounds labeled in the figure correspond to Table 1.

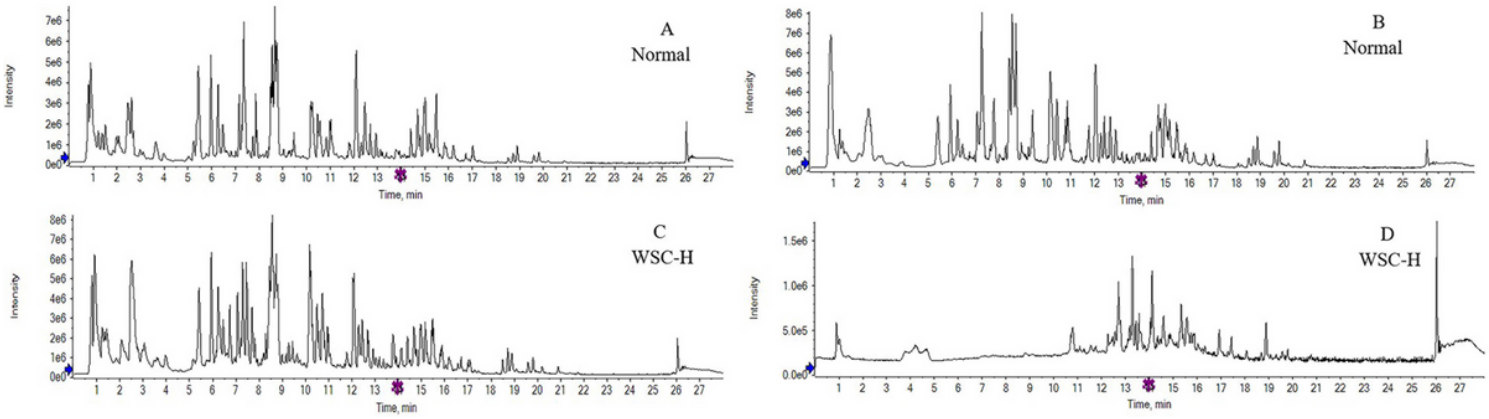

Figure 4

Total ion chromatography (TIC) of normal and WSC serum samples obtained in negative mode after treatment with methanol and acetonitrile, respectively. **A** Total ion chromatography (TIC) of the serum samples in the normal group obtained in negative ion mode after treatment with methanol. **B** TIC of the serum samples in the normal group obtained in negative ion mode after treatment with acetonitrile. **C** TIC of the serum samples in the WSC-H group obtained in negative ion mode after treatment with methanol. **D** TIC of the serum samples in the WSC-H group obtained in negative ion mode after treatment with acetonitrile.

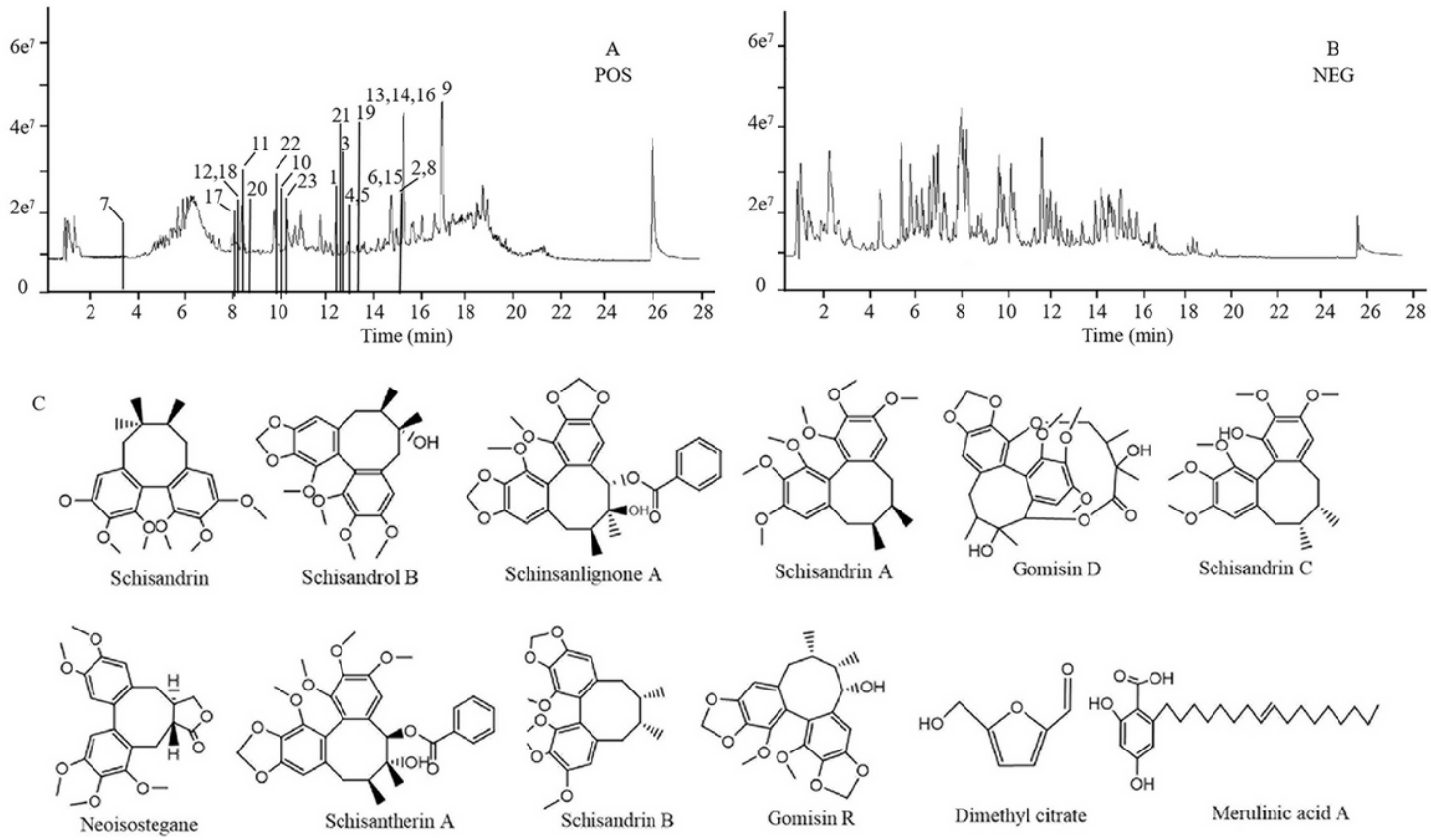

Figure 5

Identification of pharmacologically active components in serum of WSC-H group. **A** The TIC of serum samples in the WSC-H group in positive ion mode. **B** The TIC of serum samples in the WSC-H group in negative ion mode. Refer to the text for detailed analysis conditions, and the compounds labeled in the figure correspond to Table 2. **C** The structural formula of potentially bioactive compounds in serum.

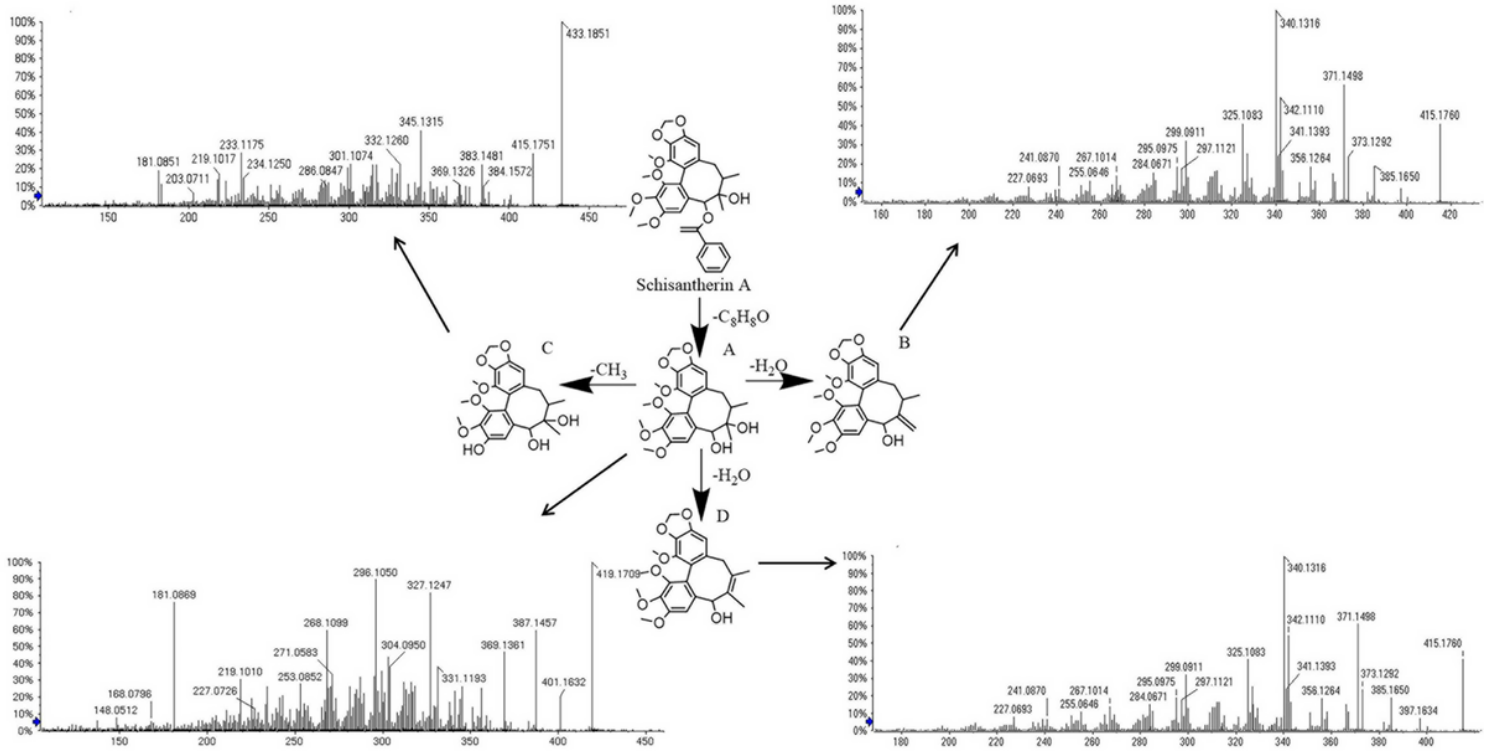

Figure 6

The proposed metabolic pathways of Schisantherin A in serum. **A** The ion fragment of 6-debenzoyl-Schisantherin A. **B** The ion fragment of 3-demethylation-6-debenzoyl-Schisantherin A. **C** The ion fragment of 7,8-dehydration-6-debenzoyl-Schisantherin A. **D** The ion fragment of 7,17-dehydration-6-debenzoyl-Schisantherin A.

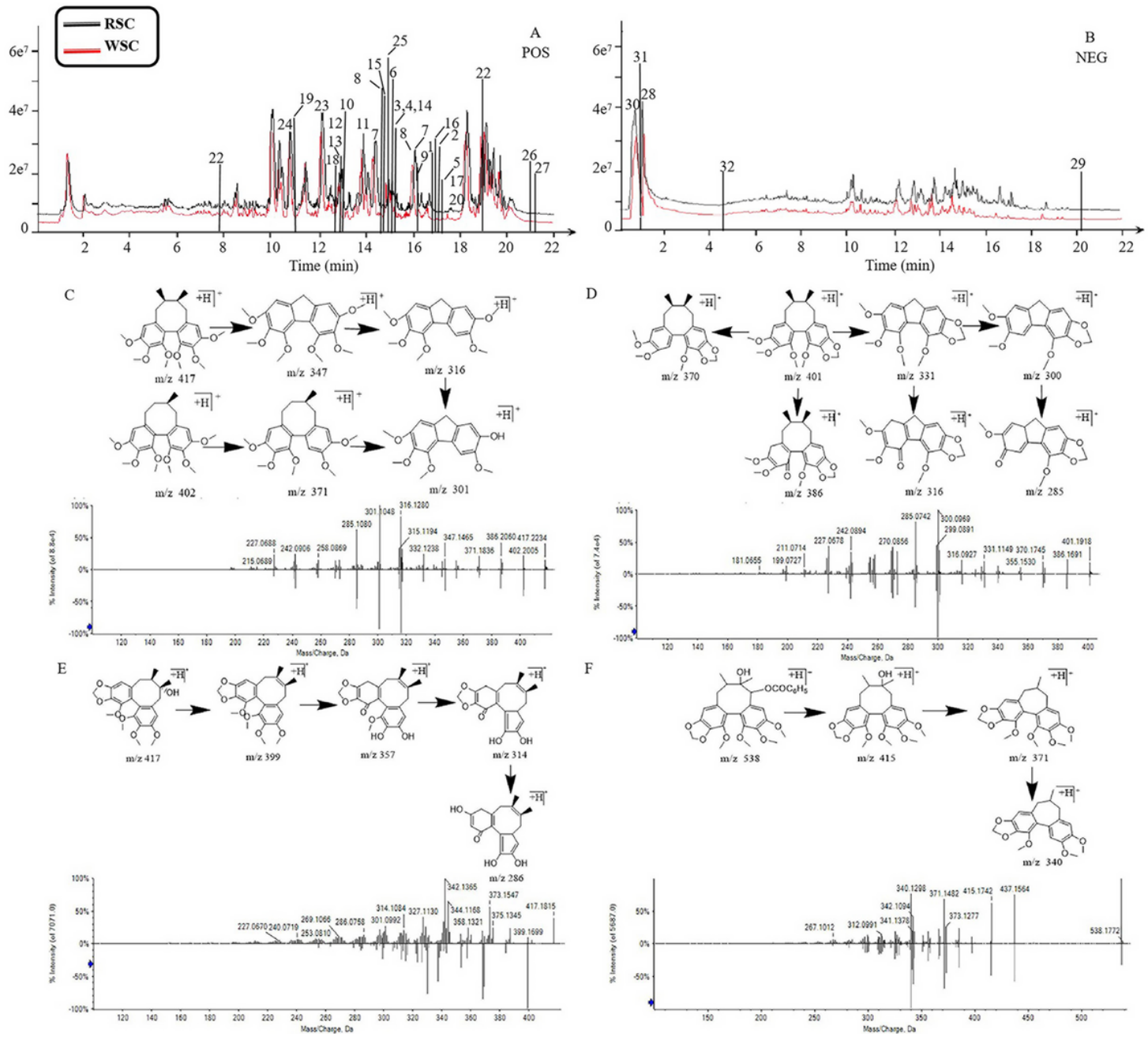

Figure 7

Identification of chemical profiles between RSC and WSC. **A** The TIC of RSC and WSC decoction in positive ion mode. **B**The TIC of RSC and WSC decoction in negative ion mode, the ingredients marked in the figure corresponding to Table 2. **C** The fragmentation pattern and secondary mass spectra of Schisandrin A. **D** The fragmentation pattern and secondary mass spectra of Schisandrin B. **E** The fragmentation pattern and secondary mass spectra of Schisandrol B. **F** The fragmentation pattern and secondary mass spectra of Schisantherin A.

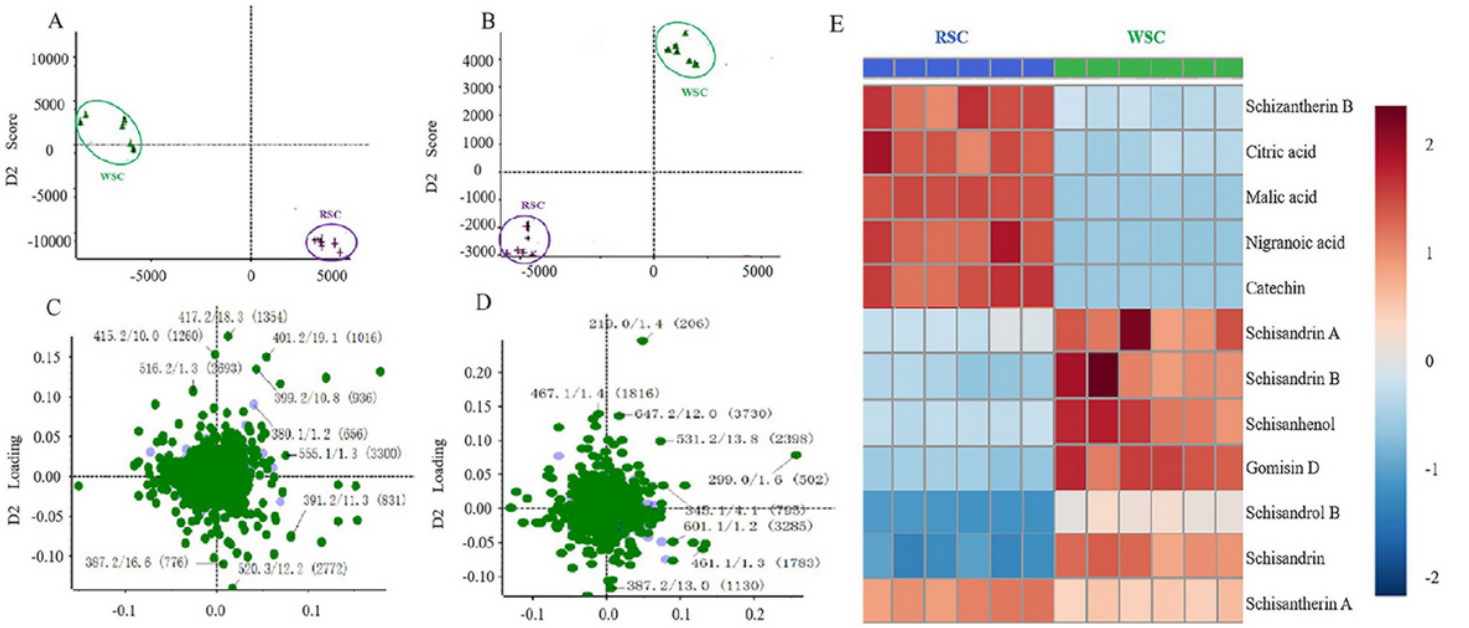

Figure 8

The PCA of RSC and WSC decoction pieces. **A**The PCA score plot of RSC and WSC decoction pieces in positive ion mode. The samples of the WSC decoction pieces were distinctly separated from the RSC decoction pieces. **B** The PCA score plot of RSC and WSC decoction pieces in negative ion mode. **C** S-plot between the decoction of RSC and WSC decoction pieces in positive ion mode. **D** S-plot between the decoction of RSC and WSC decoction pieces in negative ion mode. **E** Changes in dissolution rates of differential chemical components between RSC and WSC.The darker the red, the higher the dissolution rates, and the darker the blue, the lower the dissolution rates.

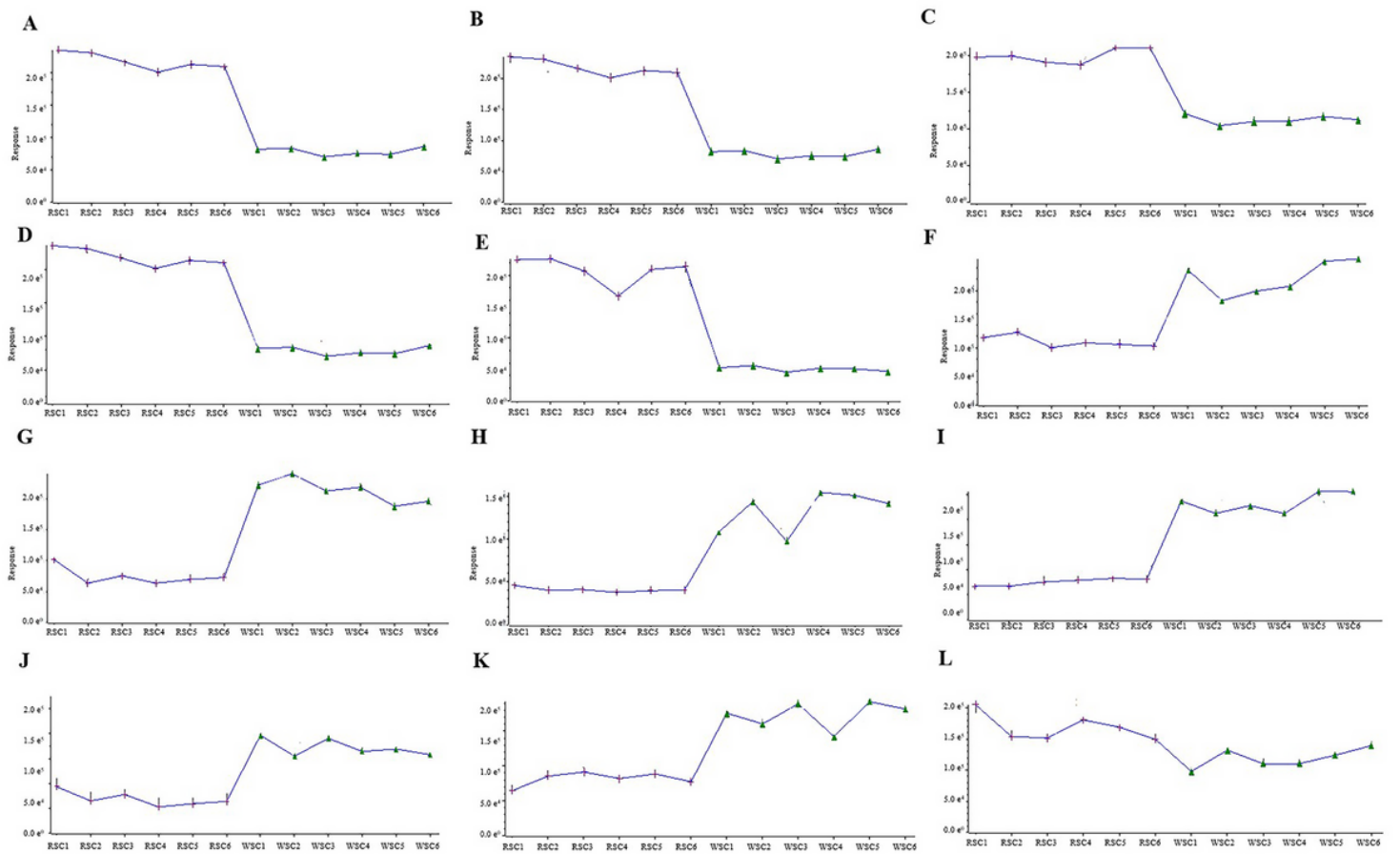

Figure 9

Content change of 12 ingredients before and after wine steaming. **A** Schizantherin B. **B** Citric acid. **C**Malic acid. **D** Nigranoic acid. **E** Catechin. **F** Schisandrin A. **G** Schisandrin B. **H** Schisanhenol. **I** Gomisin D. **J**Schisandrol B. **K** Schisandrin. **L** Schisantherin A.

Fig. 10 MTC of Schisandrin, Schisandrol B, Schisandrin A, Schisandrin B, and Gomisin D to zebrafish.

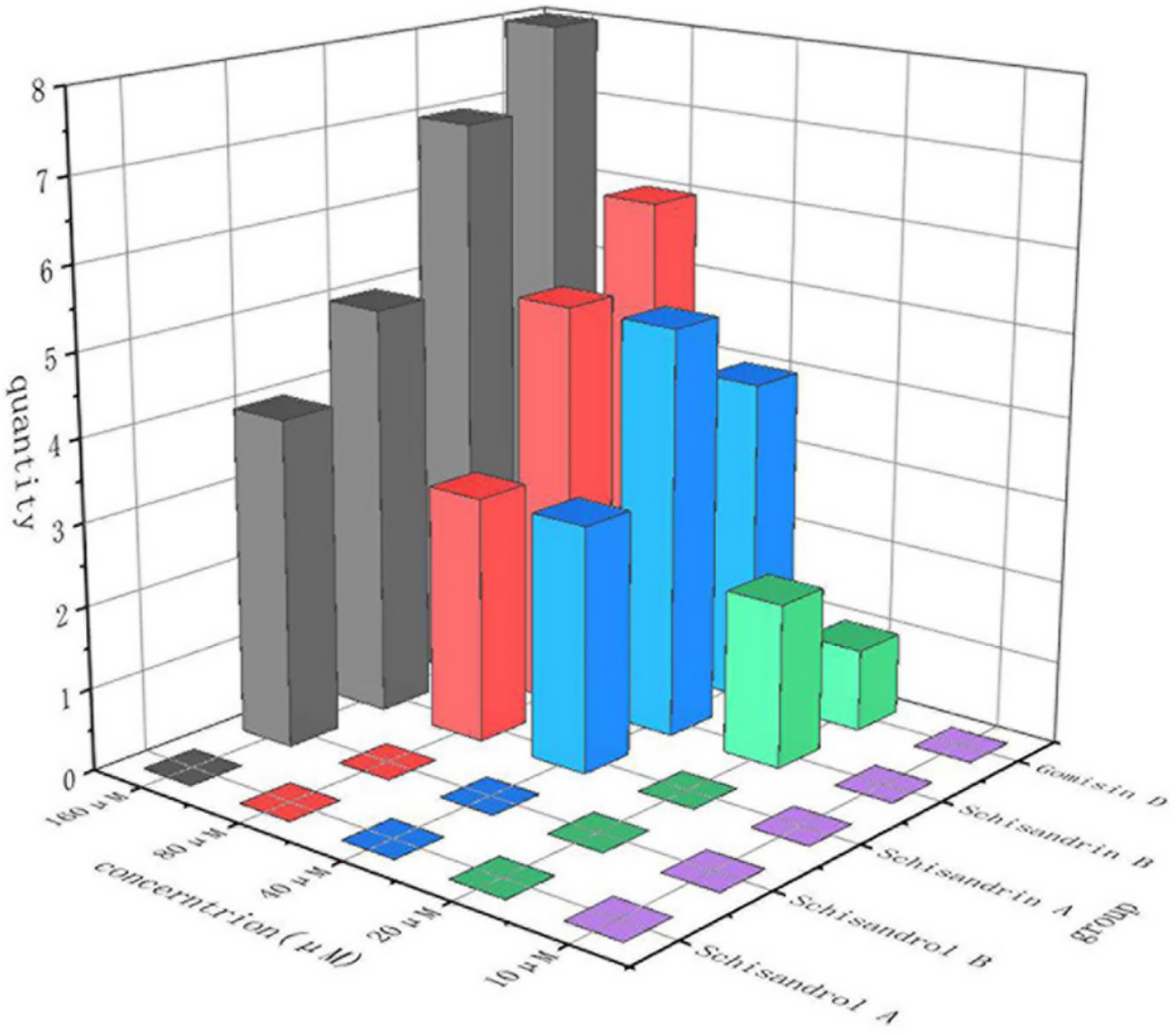

Figure 10

MTC of Schisandrin, Schisandrol B, Schisandrin A, Schisandrin B, and Gomisin D to zebrafish.

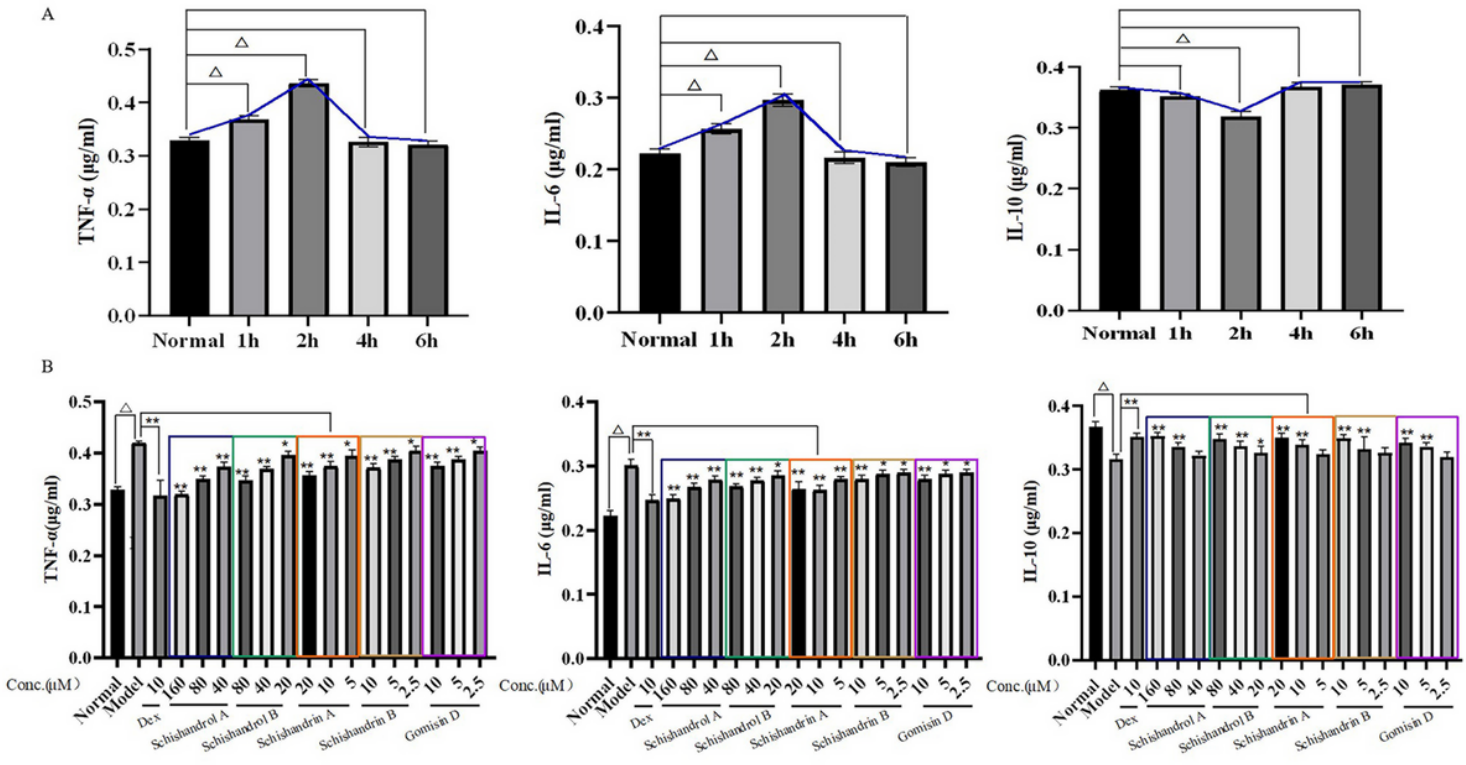

Figure 11

Efficacy validation based on zebrafish inflammatory model. **A** Screening of the optimal time points. **B** Effects of five Q-markers on TNF-α, IL-6, and IL-10. The data are expressed as mean±SD (n=10). $^{\triangle}p < 0.05$ and $^{\triangle\triangle}p < 0.01$ vs. normal group $^{*}p < 0.05$ and $^{**}p < 0.01$ vs. model group.